2003

A disjoining pressure for small contact angles and its applications

Qingfang Wu
Louisiana State University and Agricultural and Mechanical College

A DISJOINING PRESSURE FOR SMALL CONTACT ANGLES AND ITS APPLICATIONS

A Thesis
Submitted to the Graduate Faculty of the
Louisiana State University and
Agricultural and Mechanical College
in partial fulfillment of the
requirements for the degree of
Master of Science
in Mechanical Engineering

In

The Department of Mechanical Engineering

by
Qingfang Wu
B.S., Xi'an Jiaotong University, 1996
M.S., Xi'an Jiaotong University, 1999
May 2003

ACKNOWLEDGEMENTS

First of all, the author would like to thank her major professor, Dr. Harris Wong for his constant encouragement, insightful suggestions, and devoted guidance and help throughout the research and preparation of this thesis.

The author also likes to thank Dr. G. Sinclair and Dr. K. Gonthier for their time and efforts to serve on her examination committee.

The author appreciates her colleagues in lab: W. Kan, D. Min, T. Xin and J. Zhang for their help and a great time they spent together.

TABLE OF CONTENTS

LIST OF FIGURES

ABSTRACT

A thin liquid film experiences additional intermolecular forces when the film thickness h is less than roughly 100 nm. The effect of these intermolecular forces at the continuum level is captured by the disjoining pressure Π. Since Π dominates at small film thicknesses, it determines the stability and wettability of thin films. To leading order, a thin film can be treated as uniform and $\Pi = \Pi(h)$. This form, however, cannot be applied to films with non-zero contact angles. A recent ad-hoc derivation to include the slope h_x leads to a $\Pi = \Pi(h, h_x)$ that allows a contact line to move without slip. This work derives a new disjoining-pressure formula by minimizing the total energy of a drop on a solid substrate. The minimization yields an equilibrium equation that relates Π to an excess interaction potential $E = E(h, h_x)$. By considering a fluid wedge on a solid substrate, $E(h,h_x)$ is found by pairwise summation of van der Walls potentials. This gives in the small-slope limit

$$\Pi = \frac{B}{h^3}\left(\alpha^4 - h_x^4 + 2hh_x^2 h_{xx}\right),$$

where α is the contact angle and B is a material constant. The term containing the curvature h_{xx} is new; it prevents a contact line from moving without slip. Equilibrium drop and meniscus profiles are calculated for different B. Evolution of a film step is solved by a finite-difference method with the new disjoining pressure included; it is found that $h_{xx} = 0$ at the contact line is sufficient to specify the contact angle.

CHAPTER 1. INTRODUCTION

A thin fluid film may be subject to additional intermolecular forces if the thickness is less than roughly 100 nm. These forces can come from various sources, such as electrostatic or dipole-dipole interactions or a combination of the two (Israelachvili 1992). An uncharged and non-polar molecule has an instantaneous dipole that can induce polarization on others to create a net attraction between molecules. This gives rise to dispersion forces that usually are the main contribution to the van der Waals force (Israelachvili 1992, Mahanty & Ninham 1976). Before the advance of atomic force microscopes, intermolecular forces are usually studied by pressing a bubble against a solid surface. A uniform thin film forms for some liquid-solid systems. The film can sustain compression and its thickness decreases with increasing pressure. By varying the bubble pressure, the disjoining pressure Π in the film can be measured as a function of film thickness h. Similar measurements can be made on a freely-suspended liquid film supported on a solid frame. Nowadays, intermolecular forces between solid-solid surfaces are routinely measured by atomic force microscopes. Owing to the historic development, thin-film forces per unit area are commonly referred to as the disjoining pressure.

The disjoining pressure dominates at small film thicknesses, and therefore governs the stability and wettability of thin films. For example, the exposed part of the eyeball is protected by a tear film, which is deposited by the rising meniscus of the upper lid during a blink (Wong et al. 1996). After deposition, a

tear film thins rapidly near the lid meniscus and may breakup before the next blink if the disjoining pressure is destabilizing. Repeated rupture of the tear film may cause epithelium desiccation and corneal ulceration. In the lung, airways are lined with a liquid film. Normal lungs produce surfactants to reduce the surface tension of the liquid film. Insufficient surfactants can lead to respiratory difficulties caused by closure of small airways. An effective treatment for surfactant deficiency is to inhale surfactant-laden aerosols. As a surfactant droplet spreads on a liquid film, a shock forms followed by a thin region, which may break in a finite time if the disjoining pressure is destabilizing (Jensen & Grotberg 1992). Thin-film forces can also control the wettability of solid surfaces. A water-wet surface covered by a water film has a stabilizing disjoining pressure. However, if the non-wetting phase is asphaltic oil with high-molecular-weight aggregates, and if the water film is pressed very thin, then the asphaltene aggregates can adsorb irreversibly onto the solid surface and change it into oil-wet. On an oil-wet surface, an oil film is stable whereas a water film is not. Thus, the disjoining pressure has been altered. This irreversible alteration can explain the geological development of mixed wettability in oil-reservoir rock (Kovscek et al. 1993). A drainage model based on the irreversible alteration reproduces a range of phenomena associate with oil recovery from mixed-wet porous media. Given the importance of disjoining pressure in biological and industrial processes, it is critical that an accurate model of disjoining pressure be developed.

Since thin films are generally flat, the disjoining pressure can be taken to leading order as a function of film thickness only: $\Pi = \Pi(h)$. For dispersion forces, this leads to $\Pi = A/6\pi h^3$, where A is the Hamaker constant. This form has been applied to films with non-zero slopes. It has even been extended to model film breakup and spreading in which the film thickness $h \to 0$. Since this disjoining pressure contains h^{-3} and is highly singular as $h \to 0$, its validity in modeling non-zero contact angles has been questioned.

Hocking(1993) attempted to rectify this deficiency. He extended the results of Miller & Ruckenstein (1974), who considered a liquid wedge on a solid substrate and calculated the intermolecular potential Φ^* at a point on the liquid-vapor interface assuming van der Waals interactions between liquid-liquid and liquid-solid molecules and neglecting vapor contribution. They found that Φ^* is constant along the liquid-vapor interface at a particular wedge angle ψ. The constancy of Φ^* is used as the equilibrium condition, and ψ is taken as the equilibrium contact angle. Hocking (1993) took $\Pi = \Phi^*$, and allowed the slope of the wedge h_x to be different from the equilibrium value. In the small-slope limit, he got

$$\Pi = -\frac{B^*}{h^3}\left(\psi^4 - h_x^4\right), \tag{1.1}$$

where B^* and ψ depend on the van der Waals potentials and number densities. There are two problems with this derivation. First, Φ^* equal constant

at the interface does not imply equilibrium because Φ^* still varies inside the liquid wedge. Second, taking $\Pi = \Phi^*$ is unjustified.

In this work, equilibrium conditions are derived by minimizing the total energy of a drop on a substrate that includes an excess interaction potential energy E between liquid and solid (Chapter 2). This potential energy is assumed to depend on both the film-height h and film-slope h_x. The minization yields the augmented Young-Laplace equation, in which

$$\Pi = -\frac{\partial E}{\partial h} + \frac{d}{dx}\left(\frac{\partial E}{\partial h_x}\right), \tag{1.2}$$

where x is a coordinate along the solid surface. To find $E = E(h,h_x)$, we again consider a liquid wedge on a substrate and calculate the intermolecular potential Φ at a point in the liquid (Chapter 3). We argue that

$$E = \int_0^h (\Phi - \Phi_\infty) dy, \tag{1.3}$$

where Φ_∞ is the bulk value of Φ far from the solid substrate, and y is a coordinate normal to the solid surface. This gives

$$\Pi = -\frac{B}{h^3}\left(\alpha^4 - h_x^4 + 2hh_x^2 h_{xx}\right), \tag{1.4}$$

where α is the contact angle and B is a material constant given in (3.5b) and (3.5c). This equation differs from Hocking's in that a higher-order term appears and the contact angle α is no longer the wedge angle. Hocking's disjoining pressure allows a contact line to move without slip. With the higher-order term,

a contact line cannot move in the absence of slip which agrees better with physical evidence.

The new disjoining pressure is used to solve equilibrium drop and meniscus shapes in Chapter 4. Beside recovering the solutions for $\Pi = A/6\pi h^3$, a new class of shapes is found, such as planar wedges, curved wedges, and drops, that is made possible by the slope-dependent disjoining pressure. Evolution of a semi-infinite uniform film is simulated numerically in Chapter 5. We show that the contact line cannot move without slip when the new disjoining pressure is included in the evolution equation. The model problem also illustrates the proper boundary conditions at the contact line. The linear stability of uniform films is studied in Chapter 6. Further discussion and conclusions are provided in Chapter 7.

CHAPTER 2. MINIMIZATION OF THE TOTAL ENERGY

Consider a two-dimensional liquid drop on a smooth solid surface and in equilibrium with its own vapor, as illustrated in Fig. 1. This system has surface energies and an excess interaction potential energy per unit area, E, due to thin-film forces. At equilibrium, the system's total energy is at a minimum and its variation is zero:

$$\delta\int_0^{x_0}[\sigma\sqrt{1+h_x^2}+\sigma_{fs}-\sigma_{sg}+E+p_c h]dx=0\,, \tag{2.1}$$

where δ is the variation operator, h is the film height, x is a horizontal coordinate starting at the center of the drop, $h_x = dh/dx$, σ is the liquid-vapor surface tension, σ_{fs} and σ_{sg} are the liquid-solid and solid-vapor surface tensions respectively, and x_0 is the half width of the drop. Owing to symmetry, only half of a drop is considered. The first term in the integral represents the surface energy of the liquid-vapor interface. The second and third represent the net surface energy at the liquid-solid interface; if the liquid-solid interface lengthens, then the system gains liquid-solid surface energy but loses solid-vapor surface energy. Conservation of mass is imposed via a Lagrange multiplier p_c. The excess interaction potential energy E is a function of both film thickness and film slope: $E = E(h,h_x)$. Expansion of (2.1) gives

$$\int_0^{x_0}\left(\frac{\partial E}{\partial h}+p_c\right)(\delta h)dx+\int_0^{x_0}\left(\frac{\sigma h_x}{\sqrt{1+h_x^2}}+\frac{\partial E}{\partial h_x}\right)(\delta h_x)dx$$
$$+\left(\sigma\sqrt{1+h_x^2}+\sigma_{fs}-\sigma_{sg}+E\right)\Big|_{x_0}\delta x_0=0, \tag{2.2}$$

where the drop-edge position is allowed to vary (by δx_0). Since $\delta h_x = d(\delta h)/dx$, the second integral is expanded via integration by parts

$$\int_0^{x_0}\left(\frac{\partial E}{\partial h}+p_c-\frac{\sigma h_{xx}}{\left(1+h_x^2\right)^{3/2}}-\frac{d}{dx}\left(\frac{\partial E}{\partial h_x}\right)\right)\delta h dx-\left(\frac{\sigma h_x}{\sqrt{1+h_x^2}}+\frac{\partial E}{\partial h_x}\right)\delta h\Big|_{x=0}$$
$$+\left(\frac{\sigma}{\sqrt{1+h_x^2}}+\sigma_{fs}-\sigma_{sg}+E-h_x\frac{\partial E}{\partial h_x}\right)\Big|_{x=x_0}\delta x_0=0, \tag{2.3}$$

where $\delta h\big|_{x=x_0}=-h_x\,\delta x_0\big|_{x=x_0}$. Since δh is arbitrary, the above equation yields three conditions that govern the equilibrium shape of a drop on a solid surface.

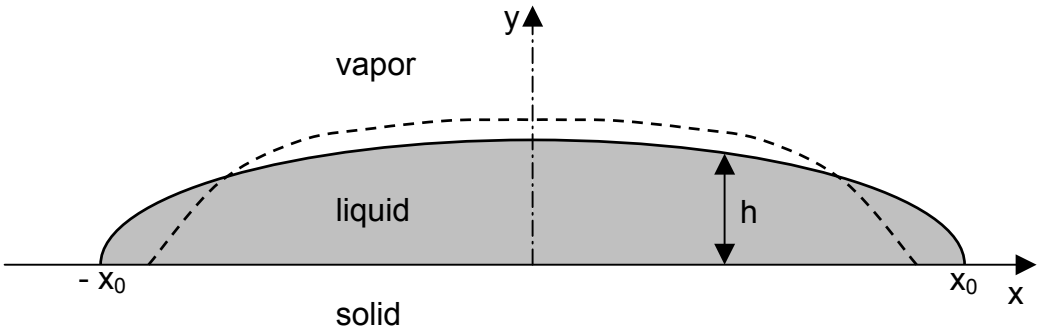

Figure 1. A two-dimensional drop on a solid substrate.

The first coefficient leads to the augmented Young-Laplace equation in two dimensions:

$$\frac{\sigma h_{xx}}{\left(1+h_x^2\right)^{3/2}}-\frac{\partial E}{\partial h}+\frac{d}{dx}\left(\frac{\partial E}{\partial h_x}\right)=p_c. \tag{2.4}$$

By comparing with the usual augmented Young-Laplace equation, a disjoining

pressure Π can be defined as

$$\Pi = -\frac{\partial E}{\partial h} + \frac{d}{dx}\left(\frac{\partial E}{\partial h_x}\right), \tag{2.5}$$

and the Lagrange multiplier p_c is recognized as the difference between the vapor pressure p_g and the liquid pressure p_f:

$$p_c = p_g - p_f . \tag{2.6}$$

The second and third terms in (2.3) serve as boundary conditions for the augmented Young-Laplace equation. At $x = 0$,

$$\frac{\sigma h_x}{\sqrt{1+h_x^2}} + \frac{\partial E}{\partial h_x} = 0 \tag{2.7}$$

At $x = x_0$,

$$\frac{\sigma}{\sqrt{1+h_x^2}} + \sigma_{fs} - \sigma_{sg} + E - h_x \frac{\partial E}{\partial h_x} = 0 . \tag{2.8}$$

At this stage of the derivation, the slope h_x need not be small. The above equations reduce to that of Yep et al. (1999) if $E = E(h)$ only. To complete the derivation, it remains to find an expression for the excess interaction potential E.

CHAPTER 3. A DISJOINING PRESSURE FOR SMALL CONTACT ANGLE

To derive an expression for $E = E(h,h_x)$, we consider a liquid wedge on a solid substrate as shown in Fig. 2. The liquid wedge is in equilibrium with its vapor. A liquid molecule M interacts with another molecule N in liquid(f), solid(s), or vapor(g) through the van der Waals potential,

$$\phi_{ff} = \frac{-\beta_{ff}}{MN^6},\ \phi_{fs} = \frac{-\beta_{fs}}{MN^6},\ \phi_{fg} = \frac{-\beta_{fg}}{MN^6}. \tag{3.1}$$

The distance between M and N is denoted by MN, and β_{ff}, β_{fs}, and β_{fg} are the strengths of the van der Waals potentials. By summing the potential between M and other liquid, solid, and vapor molecules, we find the total intermolecular potential per unit volume at point M as (Appendix A)

$$\Phi = \frac{\pi n_f^2 \beta_{ff}}{6}\left[\frac{a_1(1-\rho)+\rho-\lambda}{v_1^3} + \frac{a_2(1-\rho)}{v_2^3}\right], \tag{3.2}$$

$$\lambda = \frac{n_s \beta_{fs}}{n_f \beta_{ff}}, \tag{3.3a}$$

$$\rho = \frac{n_g \beta_{fg}}{n_f \beta_{ff}}. \tag{3.3b}$$

$$v_1 = R\sin\gamma, \tag{3.3c}$$

$$v_2 = R\sin(\psi-\gamma), \tag{3.3d}$$

$$a_1 = \frac{1}{2} - \frac{1}{4}\cos^3\gamma + \frac{3}{4}\cos\gamma, \tag{3.3e}$$

$$a_2 = \frac{1}{2} - \frac{1}{4}\cos^3(\psi-\gamma) + \frac{3}{4}\cos(\psi-\gamma), \tag{3.3f}$$

where n_f, n_s, and n_g are the number densities of liquid, solid, and vapor, v_1 is the height of molecule M, and v_2 is the distance between M and the wedge surface (Fig. 2). The wedge angle ψ will later yield the wedge slope h_x, and R and γ locate the position of M (Fig. 2). The expression of Φ in (3.2) holds for $\psi < 90^\circ$.

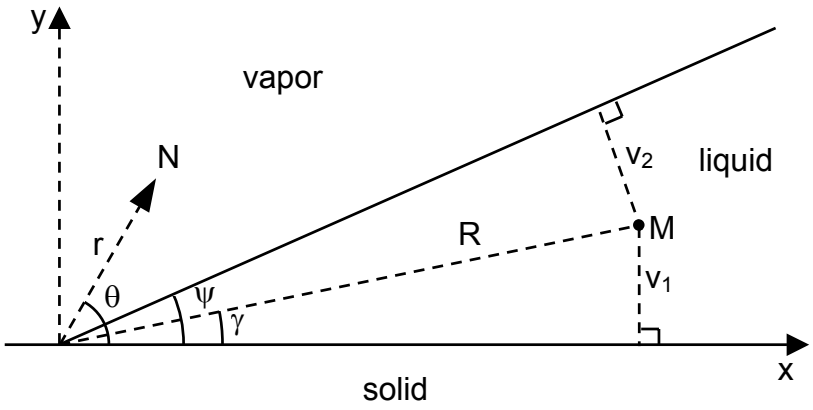

Figure 2. A liquid wedge on a solid substrate in equilibrium with its vapor.

The potential Φ is related to E in two steps. First, the bulk component Φ_∞ must be subtracted from Φ because Φ accounts for all intermolecular interactions including both bulk and thin-film components, whereas E is an excess interaction energy due to thin-film forces. The bulk component is the value of Φ far form the solid substrate, i.e., as v_1 tends to infinity but keeping v_2 fixed (Fig. 2):

$$\Phi_\infty = \frac{\pi n_f^2 \beta_{ff}(1-\rho)}{6v_2^3}. \qquad (3.4)$$

Second, Φ is energy per unit volume and varies with (x, y) (see Fig. 2), whereas E is energy per unit substrate area and depends only on x, Thus, we take

$$E = \int_0^h (\Phi - \Phi_\infty) dy . \tag{3.5}$$

Evaluation of the integral and taking the limit $h_x \to 0$ gives (Appendix B)

$$E = -\frac{\pi n_f^2 \beta_{ff} (1-\rho)}{64 h^2} \left(\frac{16}{3} \left(\frac{1-\lambda}{1-\rho} \right) + h_x^4 \right), \tag{3.6}$$

This excess energy E holds for a liquid wedge with constant slope h_x. However, the liquid drop in Fig. 1 has variable slopes. Application of E to the drop is therefore an approximation that becomes increasingly accurate as the drop edge is approached. Since the edge is where intermolecular forces become important, we deem this approximation acceptable.

Following the derivation in Chapter 2, the disjoining pressure is given as

$$\Pi = -\frac{\partial E}{\partial h} + \frac{d}{dx} \left(\frac{\partial E}{\partial h_x} \right) = -\frac{B}{h^3} \left(\alpha^4 - h_x^4 + 2 h h_x^2 h_{xx} \right). \tag{3.7a}$$

$$B = \frac{3\pi n_f^2 \beta_{ff} (1-\rho)}{32}, \tag{3.7b}$$

$$\alpha = \frac{2}{\sqrt{3}} \left(\frac{1-\lambda}{1-\rho} \right)^{1/4} . \tag{3.7c}$$

If a liquid film is flat, $h_x = h_{xx} = 0$, and (3.7a) becomes

$$\Pi = -\frac{B\alpha^4}{h^3}, \tag{3.8}$$

which recovers the usual h^{-3} dependence of the disjoining pressure. The negative sign indicates that Π in (3.8) is an attractive disjoining pressure. This follows from the long-range attractive intermolecular potential used in deriving E. However, the disjoining pressure can be positive or negative (Israelachvili 1992). To explore all possible applications, we study both positive and negative disjoining pressures. Thus, (3.7a) reads

$$\Pi = \pm \frac{B}{h^3}\left(\alpha^4 - h_x^4 + 2hh_x^2 h_{xx}\right) \tag{3.9}$$

with $B > 0$ and the positive (negative) sign representing the positive (negative) disjoining pressure.

The new disjoining pressure allows a liquid film to end at a solid substrate with contact angle $\alpha << 1$. As the film height $h \to 0$, Π can remain bounded if $h_x \to \alpha$ and $hh_{xx} \to 0$ faster than or at the same rate as $h^3 \to 0$. As shown in the next chapter, this is realized if as $x \to x_0$ (x_0 is the position of the contact line),

$$h \to \alpha(x - x_0) + O(x - x_0)^4. \tag{3.10}$$

Thus the intermolecular forces make the interface very planar near the contact line. The parameter α is identified as the contact angle. Since it is assumed $h_x << 1$ in the derivation of E, $\alpha << 1$.

The new disjoining pressure differs from that of Hocking's. Our expression contains a higher derivative h_{xx} that arises from assuming $E = E(h, h_x)$ instead of just $E = E(h)$. Thus, even if we are aiming to include only the effect of the

slope h_x, a curvature term appears and cannot be avoided. This curvature term plays a decisive role in preventing a contact line from moving without slip, as detailed in Chapter 5.

CHAPTER 4. EQUILIBRIUM FILM PROFILES

4.1 Introduction

The augmented Young-Laplace equation in two dimensions follows from (2.4)

$$\sigma h_{xx} \pm \frac{B}{h^3}\left(\alpha^4 - h_x^4 + 2hh_x^2 h_{xx}\right) = p_c . \tag{4.1}$$

This equation holds for small slopes. The pressure difference $p_c = p_g - p_f$ between the vapor pressure p_g and the liquid pressure p_f can be either positive or negative depending on the application. Equation (4.1) states that the capillary pressure σh_{xx} and the disjoining pressure must sum to a constant. Away from the contact line, the capillary pressure dominates. As $x \to x_0$, where x_0 is the position of the contact line, the disjoining pressure dominates, and (4.1) gives

$$h \to \alpha(x - x_0) \pm \frac{p_c}{8B}(x - x_0)^4 + \cdots\cdots . \tag{4.2}$$

The sign of the higher-order term corresponds to the sign of the disjoining pressure.

Minimization of the total energy leaves two boundary conditions for the drop shape, one at the symmetry plane $x = 0$ and one at the contact line $x = x_0$. Both (2.7) and (2.8) contain $\partial E / \partial h_x (= \pm 2Bh_x^3 / 3h^2)$. Equation (2.7) gives at $x = 0$,

$$h_x = 0, \tag{4.3}$$

which is simply the symmetric condition. At $x = x_0$, $E - h_x \partial E / \partial h_x = \pm B(\alpha^4 - h_x^4)/2h^2 = 0$ according to the expansion in (4.2). Thus (2.8) recovers the usual force balance in the horizontal direction at $x = x_0$:

$$\frac{\sigma}{\sqrt{1+h_x^2}} + \sigma_{fs} - \sigma_{sg} = 0. \tag{4.4}$$

This equation holds for arbitrary h_x and is recognized as Young's equation. In the derivation of Yeh et al (1999), $E = E(h)$ only, and Young's equation is not recovered because of the extra term in (2.8). This is acceptable in their formulation since the liquid film is not allowed to contact the substrate due to the singularity in $E(h)$, and there is no contact line. Here, the liquid film can contact the substrate. By assuming $E = E(h, h_x)$, two extra terms appear in (2.8), but they cancel at the contact line. This suggests that the current derivation of Π is self-consistent. Validity of Young's equation has been examined in other aspects. Equation (4.4) can determine the contact angle $\alpha = h_x(x_0) << 1$ if σ, σ_{fs} and σ_{sg} are specified. Hence, for the rest of this paper, α is assumed known.

The augmented Young-Laplace equation can be made dimensionless by a film height h_0:

$$H = \frac{h}{h_0}, \tag{4.5a}$$

$$X = \frac{\alpha x}{h_0}, \tag{4.5b}$$

$$H_{XX} \pm \varepsilon\left(\frac{1 - H_X^4 + 2HH_X^2 H_{XX}}{H^3}\right) = C, \tag{4.6}$$

$$\varepsilon = \frac{B\alpha^2}{\sigma h_0^2}, \tag{4.7}$$

$$C = \frac{p_c h_0}{\sigma\alpha^2}, \tag{4.8}$$

where C is the non-dimensional pressure difference, and ε measures the ratio of disjoining to capillary forces which is small in most applications. This equation can be integrated once to give

$$H_X^2 = \frac{\pm 1}{2\varepsilon}\left(-H^2 + \sqrt{H^4 \pm 8\varepsilon C H^3 \pm 4K\varepsilon H^2 + 4\varepsilon^2}\right), \tag{4.9}$$

where K is an integration constant. Although the square root may also take on a negative sign, only the positive sign yields physical solutions. If the liquid film touches the substrate, (4.9) gives that as $H \to 0$,

$$H_X^2 \to \pm 1. \tag{4.10}$$

Thus, only the positive disjoining pressure is physically acceptable if a film contacts the substrate. Furthermore, as $H \to 0$, the only value of K in (4.9) that allows $(1 - H_X^4)/H^3$ in (4.6) to be bounded is

$$K = 1. \tag{4.11}$$

The dimensionless pressure difference C can be zero, negative, or positive depending on the application. These three cases are considered.

4.2 Equilibrium Profiles for $C = 0$

If the liquid film touches the substrate, then $K = 1$ in (4.9) and the disjoining pressure must be positive. Thus, (4.9) reduces to

$$H_X^2 = 1. \tag{4.12}$$

Hence, the film is a wedge with slope ± 1. This wedge solution holds for arbitrary ε. Since the derivation of Φ uses a wedge film, recovery of the wedge solution shows self-consistency.

If the liquid film does not touch the substrate, then it must have one symmetric plane since (4.6) is invariant by changing X to $-X$. (The uniform-film solution is excluded by (4.6).) The film height h_0 at the symmetric plane provides a length scale: at $X = 0$, $H = 1$, and $H_X = 0$. This forces $K = -(\pm\varepsilon)$ in (4.9). However, K must be positive since in the limit $H \to \infty$, (4.9) gives

$$H_X^2 \to K. \tag{4.13}$$

Thus, only the negative disjoining pressure is acceptable and the symmetric condition yields

$$K = \varepsilon. \tag{4.14}$$

For $\varepsilon << 1$, the film is mildly inclined because $H_X \to \varepsilon^{1/2}$ as $H \to \infty$. The film profiles can be normalized by defining

$$\varsigma = \varepsilon^{1/2} X. \tag{4.15}$$

Equation (4.13) gives that as $H \to \infty$,

$$H_\varsigma \to 1. \tag{4.16}$$

Equation (4.6) for the negative disjoining pressure becomes

$$H_{\varsigma\varsigma} - \left(\frac{1 - \varepsilon^2 H_\varsigma^4 + 2\varepsilon^2 H H_\varsigma^2 H_{\varsigma\varsigma}}{H^3} \right) = 0 , \tag{4.17}$$

This equation is solved numerically by a fourth-order Runge-Kutta method, and the computed profiles are plotted in Fig. 3 for various ε.

Since ε^2 appears in the transformed equation, the solution is insensitive to ε for $\varepsilon << 1$. An asymptotic solution is found for (4.17) in the limit $\varepsilon \to 0$ (Appendix C):

$$H(\varsigma) = H_0(\varsigma) + \varepsilon^2 H_1(\varsigma) + \cdots . \tag{4.18}$$

$$H_0 = \sqrt{\varsigma^2 + 1} . \tag{4.19}$$

$$H_1 = -\frac{\varsigma^2}{4(\varsigma^2 + 1)^{3/2}} \left(1 - \frac{(\varsigma^2 + 1)\tan^{-1}(\varsigma)}{\varsigma} \right) . \tag{4.20}$$

This solution is also plotted in Fig. 3. It agrees well with the numerical results even for $\varepsilon = 0.5$.

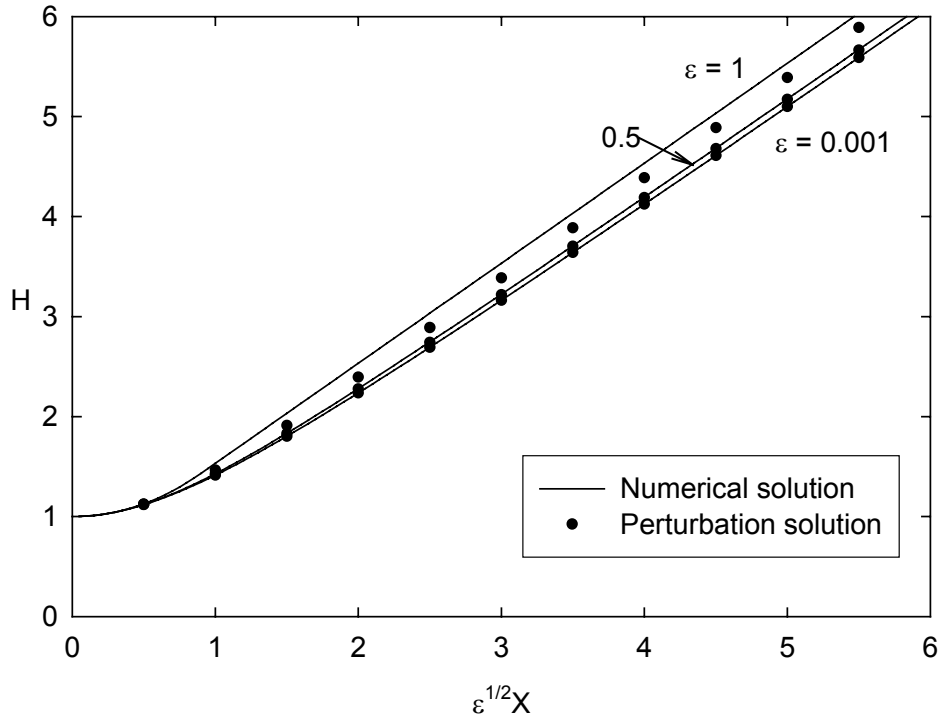

Figure 3. Symmetric film profiles for C=0 and various ε

4.3 Equilibrium Profiles for $C < 0$

If $C < 0$, the liquid pressure exceeds the vapor pressure, and two equilibrium solutions are found: a drop and a uniform film. For a drop, K=1 and the disjoining pressure is positive because the drop surface contacts the substrate. At the drop center, $h = h_0$ or $H = 1$ and symmetry demands $H_X = 0$. Thus, (4.9) gives

$$C = -\frac{1+\varepsilon}{2}. \tag{4.21}$$

Equation (4.6) is solved using a fourth-order Runge-Kutta method. The integration starts at $X = 0$ with $H = 1$ and $H_X = 0$; it stops when H becomes

zero. Computed drop profiles are plotted in Fig. 4 for various ε. If $\varepsilon = 0$, the parabolic drop shape is recovered: $H = -X^2/4 + 1$. The contact line position is $X_0 = 2$ and the volume of half a drop is $V = 4/3$. As ε increases, the liquid drop becomes more pointed (Fig. 4) and both X_0 and V decrease (Fig. 5). The profiles in Fig. 4 are non-dimensionalized such that the drop height is unity at the center and the slope is unity at the edge. In Fig. 5, the width is made dimensionless by h_0/α and the volume by h_0^2/α.

The limit $\varepsilon \to 0$ is singular and a boundary layer exists near the contact line. The singularity arises because setting $\varepsilon = 0$ in (4.6) eliminates the boundary condition at the contact line; (4.9) becomes undefined and C cannot be determined. The length scales in the inner region are found by balancing the dominant capillary pressure and disjoining pressure terms in (4.6): $\delta H \sim \delta X \sim \varepsilon^{1/2}$. The drop profile can then be solved by the method of matched asymptotic expansions (Appendix D). To leading order,

$$H = \frac{C}{2}X^2 + 1, \tag{4.22}$$

$$C = -\frac{1}{2}, \tag{4.23}$$

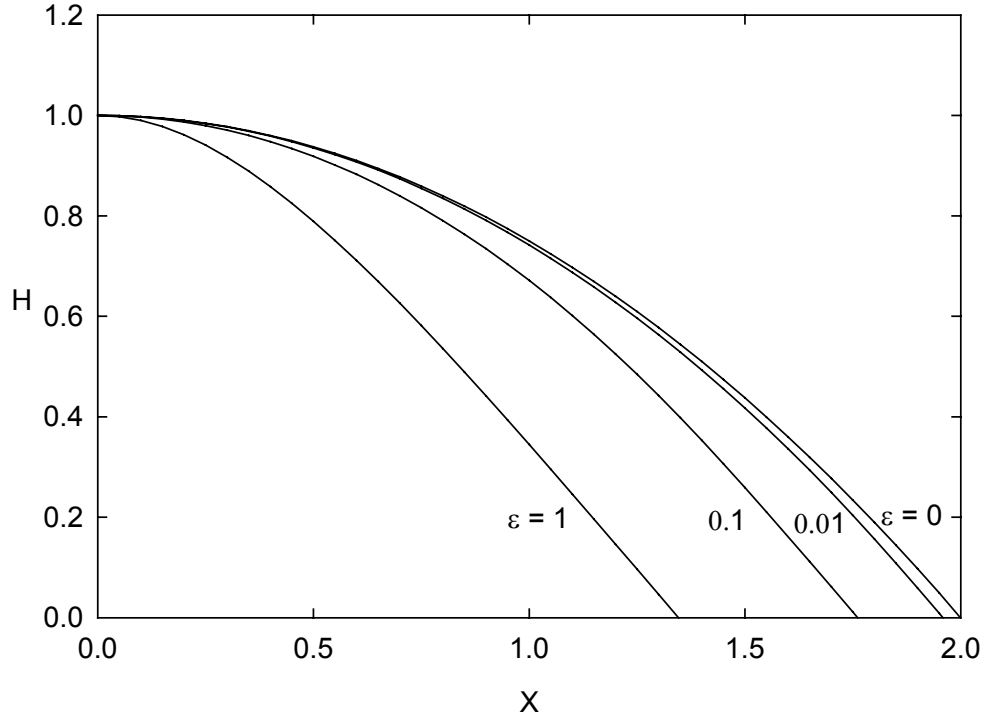

Figure 4. Equilibrium drop profiles for various ε.

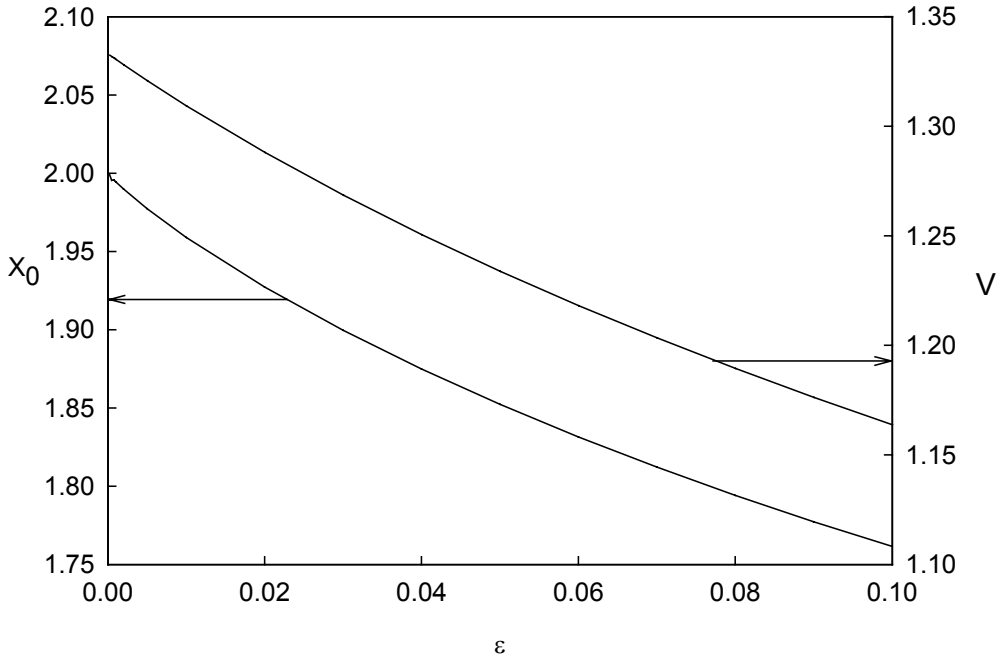

Figure 5. Half width X_0 and half volume V of a drop versus epsilon.

The asymptotic drop profile is plotted in Fig. 4 and compared with the numerical solution for $\varepsilon = 0.01$.

Equation (4.6) also admits a uniform-film solution with $H = 1$ (i.e. $h = h_0$), $H_X = 0$, and $H_{XX} = 0$. Thus, (4.6) shows that the disjoining pressure must be negative, and

$$C = -\varepsilon . \tag{4.24}$$

The conjoining pressure pulls the film together to balance the pressure difference across the film surface. The dimensional film thickness $h_0 = \left(-B\alpha^4 / p_c\right)^{1/3}$ as determined by (4.24)

4.4 Equilibrium Profiles for $C > 0$

If $C > 0$, the vapor pressure is higher than the liquid pressure, and three equilibrium solutions are found: a uniform-film, a uniform-film that grows to a constant-curvature surface (Fig. 6), and a film wedge that grows to a constant-curvature surface (Fig. 7).

A uniform-film has naturally its thickness as a length scale: $H = 1$, $H_X = 0$, $H_{XX} = 0$. Thus (4.6) gives

$$C = \varepsilon . \tag{4.25}$$

Since $C > 0$, only the positive disjoining pressure is acceptable. The above equation yields the dimensional film thickness $h_0 = \left(B\alpha^4 / p_c\right)^{1/3}$.

A uniform-film can grow in the x-direction to approach a constant-curvature surface. Deviation from the uniform-film is exponential, as shown by substituting

$H(X) = 1 + \delta(X)$ into (4.6). By assuming $\delta << 1$, the equation is linearized as

$$\delta_{XX} - 3\varepsilon\delta = 0. \tag{4.26}$$

Only the positive disjoining pressure needs to be considered as demanded by the uniform-film solution. Thus, we find

$$\delta = a_m e^{\pm(3\varepsilon)^{1/2}X}. \tag{4.27}$$

The amplitude a_m needs to be small but its value has no physical significance; different values of a_m yield the same profile except for a shift in the origin of X. As a film grows, $H >> 1$, and (4.9) shows $H_X^2 \to 2CH$ or

$$H_{XX} \to C. \tag{4.28}$$

Hence, the curvature becomes constant away from the wall. Since $C = \varepsilon$ for a uniform-film, the curvature is small for $\varepsilon << 1$. Equations (4.26) and (4.27) suggest $X \sim \varepsilon^{-1/2}$ as $\varepsilon \to 0$. Thus, the film profiles are normalized in terms of the variable $\varsigma = \varepsilon^{1/2}X$, and (4.6) becomes

$$H_{\varsigma\varsigma} + \left(\frac{1 - \varepsilon^2 H_\varsigma^4 + 2\varepsilon^2 H H_\varsigma^2 H_{\varsigma\varsigma}}{H^3} \right) = 1, \tag{4.29}$$

This equation is solved by a fourth-order Runge-Kutta method. At $\varsigma = 0$, (4.27) provides the starting conditions: $H = 1 + \delta$ and $H_\varsigma = \delta_\varsigma$ with $a_m = 0.001$. Integrated film profiles are plotted in Fig. 6 for various ε.

A film in contact with the substrate can also grow to approach a constant-curvature surface. At the contact line $X = 0$, the film grows with unit slope until $H_{XX} \to C$ as $H \to \infty$. Since there is no imposed length scale, we can take $C = 1$

(or $h_0 = \sigma\alpha^2 / p_c$). Thus, ε is the only remaining parameter. Near the contact line as $X \to 0$, (4.6) gives

$$H \to X + \frac{X^4}{8\varepsilon} + \ldots. \tag{4.30}$$

This is used to start the integration of (4.6) at $X = \Delta X = 0.01$. Calculated film profile are shown in Fig. 7 for various ε.

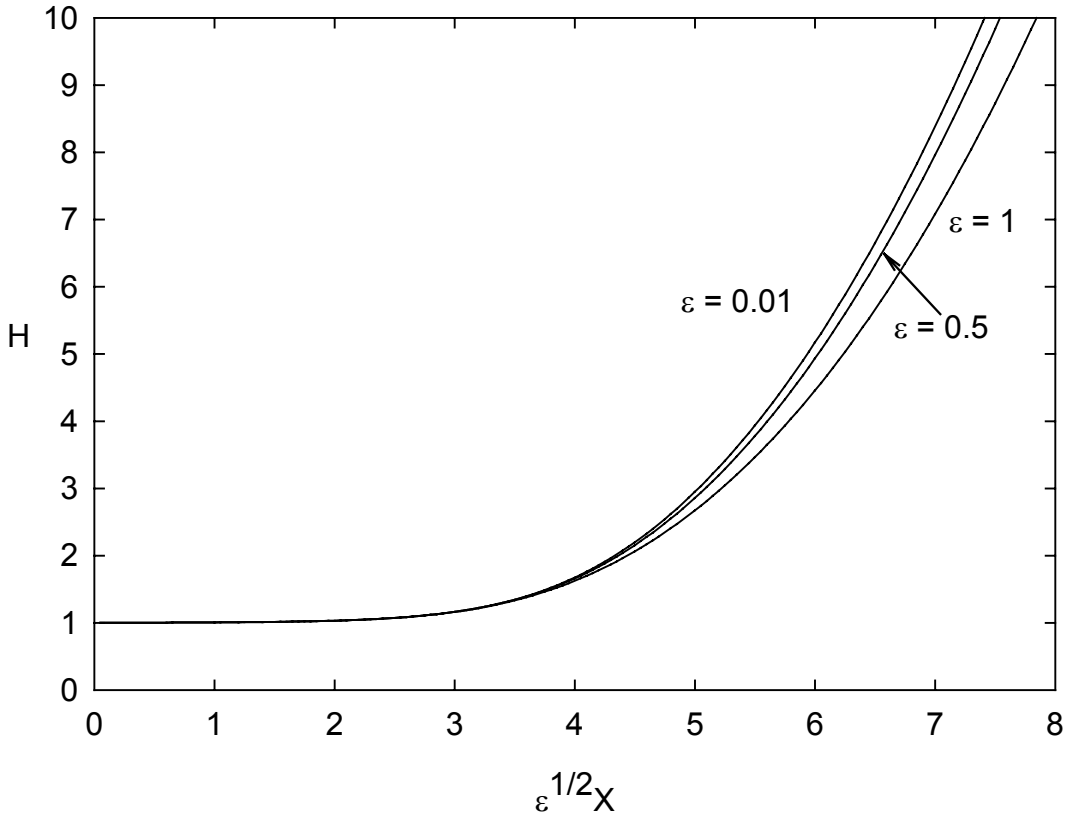

Figure 6. Uniform film grows to a meniscus.

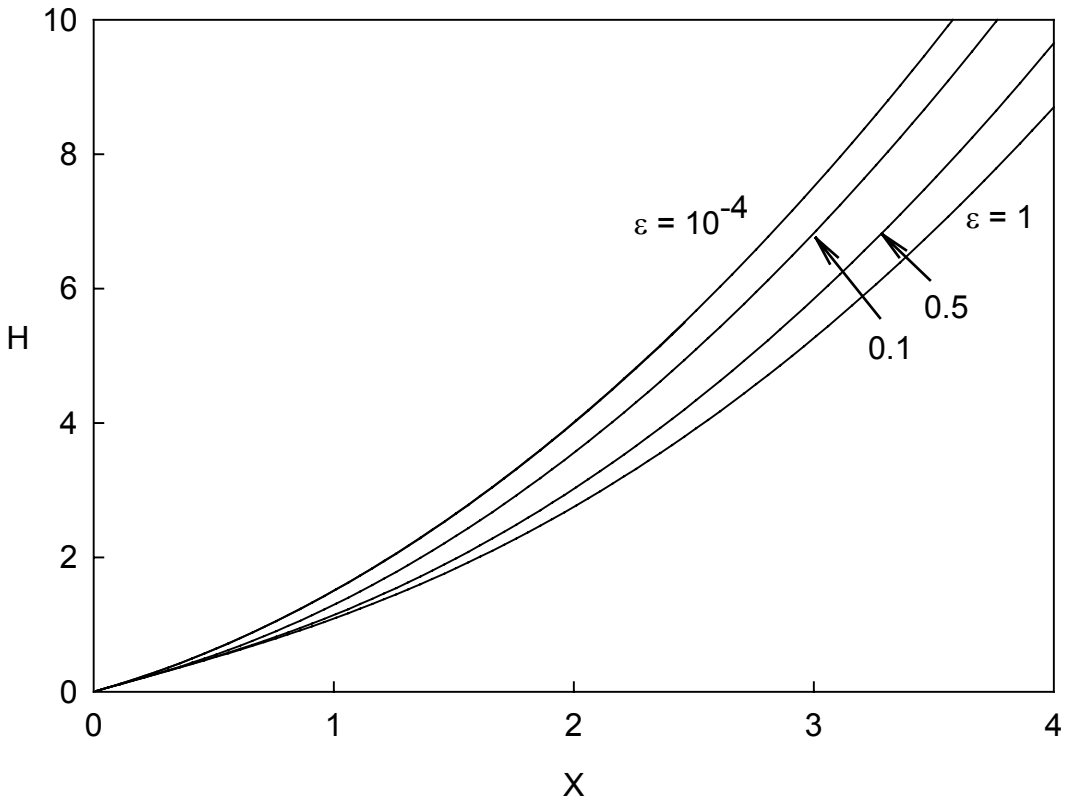

Figure 7. Contact film grows to a meniscus.

CHAPTER 5. EVOLUTION OF A FILM STEP

The augmented Young-Laplace equation in (4.1) gives the liquid pressure as

$$p_f = p_g - \sigma h_{xx} - \frac{\pm B}{h^3}\left(\alpha^4 - h_x^4 + 2hh_x^2 h_{xx}\right). \tag{5.1}$$

A liquid film of height $h(t,x)$ on a solid substrate obeys

$$\frac{\partial h}{\partial t} - \frac{1}{3\mu}\frac{\partial}{\partial x}\left(h^3\left(\frac{\partial p_f}{\partial x}\right)\right) = 0 \tag{5.2}$$

,

where t is time, x is a horizontal coordinate of the liquid. This equation assumes $h_x << 1$. A set of dimensionless variables can be defined based on the height h_0 of the uniform-film:

$$H = \frac{h}{h_0}, \tag{5.3a}$$

$$X = \frac{\alpha x}{h_0}, \tag{5.3b}$$

$$\tau = \frac{t\sigma\alpha^4}{\mu h_0}, \tag{5.3c}$$

$$\frac{\partial H}{\partial \tau} + \frac{1}{3}\frac{\partial}{\partial X}\left[H^3\frac{\partial}{\partial X}\left[H_{XX} \pm \frac{\varepsilon}{H^3}\left(1 - H_X^4 + 2HH_X^2 H_{XX}\right)\right]\right] = 0, \tag{5.4}$$

where $\varepsilon = B\alpha^2/\sigma h_0^2$. An initial profile is chosen that consists of a wedge of film near the contact line attached to a uniform film. At the contact line, $X = 0$,

$H = 0$, $H_X = 1$, and $H_{XX} = 0$. In the limit $H \to 0$, the evolution equation reduces to

$$H_\tau \pm \varepsilon 3(H_X^2 - 1)H_{XXX} = 0. \tag{5.5}$$

If $H_{XXX} = 0$ is bounded as $H \to 0$, then $H_\tau \to 0$ and the contact line cannot move. This differs from Hocking's results (see Discussion). The evolving film profile is solved numerically by finite differences. The profile is advanced in time by the backward Euler method. At each time step, the spatial derivatives are replaced by central differences, and the resulting nonlinear algebraic equations are solved iteratively by the Newton-Raphson method. At the fixed contact line $X = 0$, we set $H = 0$ and $H_{XX} = 0$. Although the slope is not specified, the evolution equation forces $H_X \approx 1$ near the contact line. At the other end of the computational domain $X = X_\infty$ the film is uniform: $H_X = 0$ and $H_{XX} = 0$.

Increasing X_∞ has no effect on the results. Computed film profiles are plotted in Fig. 8 at four different times. The parameters used in Fig. 8 are $X_\infty = 25$, $\Delta x = 0.25$, $\Delta t = 0.01$ and $\varepsilon = 0.01$.

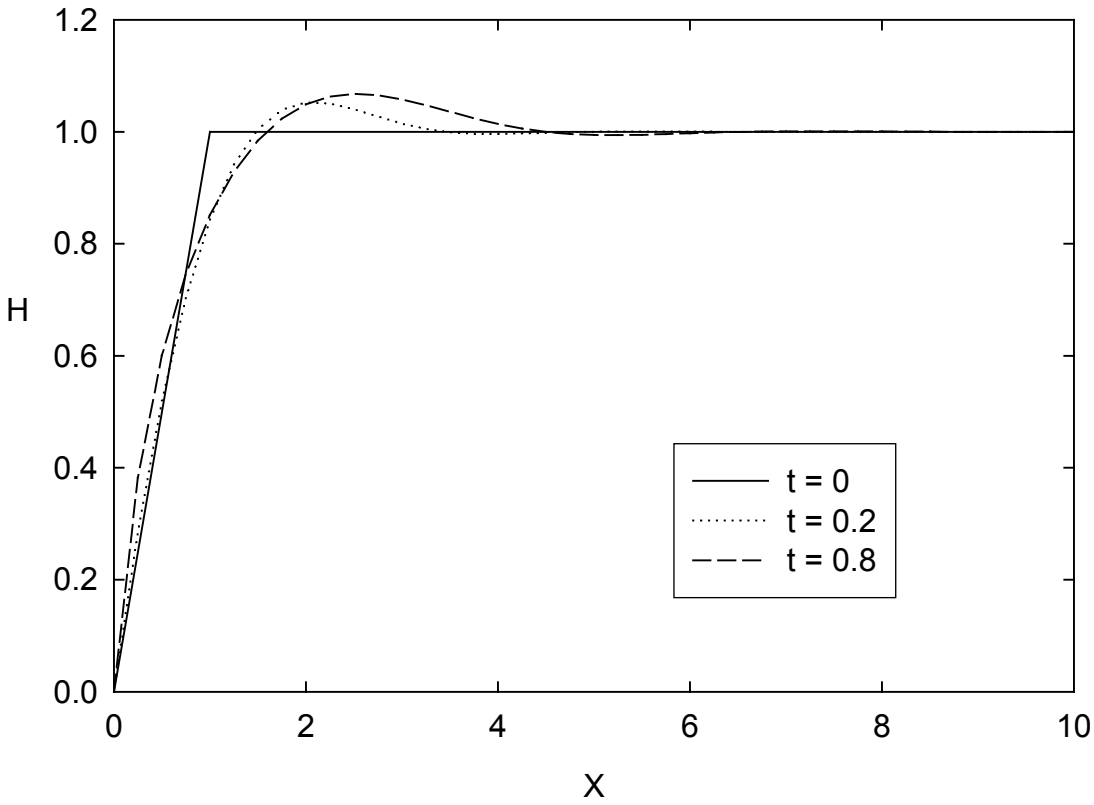

Figure 8.
Evolution profiles of the step thin film with fixed contact line at different time.

CHAPTER 6. STABILITY OF UNIFORM FILMS

The stability of the uniform-film solution $H = 1$ is studied by adding a small perturbation:

$$H(\tau, X) = 1 + \delta(\tau, X). \tag{6.1}$$

Since $|\delta| << 1$, the evolution equation can be expanded in δ. The leading order equation is linear in δ and amenable to a normal mode analysis:

$$\delta(\tau, X) = e^{\omega\tau} f(X). \tag{6.2}$$

$$\frac{d^4 f}{dX^4} - (\pm 3\varepsilon)\frac{d^2 f}{dX^2} + 3\omega f = 0, \tag{6.3}$$

The uniform-film solution holds for both positive and negative disjoining pressures. The eigenfunction is sinusoidal with wave number k:

$$f = e^{ikX}, \tag{6.4}$$

$$\omega = -\frac{k^2}{3}(k^2 \pm 3\varepsilon), \tag{6.5}$$

Thus, the uniform-film is stable if the disjoining pressure is positive. If the disjoining pressure is negative, the uniform film is stable if $k \geq (3\varepsilon)^{1/2}$, and unstable otherwise. These results are the same as those for $\Pi = \pm A / 6\pi h^3$ because the slope and curvature in the new disjoining pressure vanish for a uniform film.

CHAPTER 7. DISCUSSION AND CONCLUSIONS

-

7.1. Discussion

Surface tension results from intermolecular actions at an interface and is believed to be affected by the disjoining pressure. There is the question of how to separate the two effects since both are derived from intermolecular interactions. Some suggest that surface tension is not constant in the region where the disjoining pressure dominates. When a drop on a substrate is in equilibrium, the surface tension needs to be constant to avoid a Marangoni stress along the drop surface. In the absence of a surfactant, a Marangoni stress cannot be balanced and will always lead to fluid motion. The newly derived disjoining pressure does contain a curvature term. This term may be viewed as a form of capillary pressure introduced by the disjoining pressure. This excess capillary pressure contains h^{-2} but is actually bounded as $h \to 0$ because the curvature $h_{xx} \to 0$ and $h_{xxx} \to 0$: $2\varepsilon H_X^2 H_{XX} / H^2 \to \varepsilon H_{XXXX} = 3C$, which follows from (4.5). Thus, this excess capillary pressure is of order C near the contact line. Since $(C - \varepsilon)$ is the capillary pressure at the drop center, this excess capillary pressure is significant. In fact, the capillary pressure H_{XX} decreases as the contact line is approached and vanishes at the contact line. Thus, the pressure difference between inside and outside of the drop is balanced totally by the disjoining pressure at the contact line.

The new disjoining pressure consists of two terms: $(1-H_X^4)/H^3$ and $2H_X^2H_{XX}/H^2$. Hocking's derivation has the first term, but not the second. The second term is responsible for preventing a contact line from moving without slip. The evolution equation (5.4) reduces to (5.5) at the contact line. If $H_X^2=1$ and H_{XXX} is bounded at the contact line, then $H_\tau=0$ and the contact line cannot move. If the second term is dropped in (5.4), then as $H\to 0$,

$$H_\tau \pm \frac{2\varepsilon}{3}H_{XXX}=0. \qquad (7.1)$$

Hence, if $H_{XXX}\neq 0$, then $H_\tau \neq 0$ and the contact line moves without slip. This is responsible for Hocking's solution of a steady interfacial profile on top of an inclined plate that is sliding into a pool of liquid. He found that a steady solution exists even without slip, but not if the disjoining pressure is turned off. This conclusion is questionable because slip is needed to remove a non-integrable stress singularity at a moving contact line.

7.2. Conclusions

We have derived rigorously a new form of disjoining pressure that depends on the slope as well as the curvature of the film surface. This disjoining pressure does not allow movement of a contact line if slip is not included. This is physically sound because the disjoining pressure is a static contribution whereas slip results from dynamics. All acceptable equilibrium film profiles are calculated. For the negative disjoining pressure, the only solution is that of a uniform film. For the positive disjoining pressure, acceptable solutions include a

drop, a uniform film, a uniform film growing to a constant-curvature surface, and a wedge film growing to a constant-curvature surface. The uniform film for the negative disjoining pressure is unstable for long-wave disturbances. For the positive disjoining pressure, the uniform film is found to be linearly stable. Evolution of a film step is solved numerically by a finite-difference method. It is found that the zero curvature condition at the contact line is sufficient to maintain the contact angle.

REFERENCES

J. Mahanty, B. W. Ninham, *Dispersion Forces*, Academic Press Inc. (London) Ltd., (1976)

J. Israelachvili, *Intermolecular & Surface Forces*, Academic Press Inc. , Elsevier Science Ltd. (1992)

O. E. Jensen, J. B. Grotberg, "Insoluble surfactant spreading on a thin viscous film: shock evolution and fjilm rupture," *J. Fluid Mech.* **240**, pp259-288 (1992).

H. Wong, I. Fatt, C. J. Radke, "Deposition and Thinning of the Human Tear Film." *J.of Colloid and Interface Science.* **184**, pp44-51(1995),.

A. R. kovscek, H. Wong, and C. J. Radke, "A pore-Level Scenario for the Development of Mixed Wettability in Oil Reservoirs," *AIChE Journal.* **39(6)**, pp1072-1085(Jun 1993),.

C. A. Miller and E. Ruckenstern, "The Origin of Flow During Wetting of Solids," *J. Colloid and Interface Sci*. **48(3)**, 368 (1974).

L. M. Hocking, "The influence of intermolecular forces on thin fluid layers," *Phys. Fluids A.* **5(4)**, 793 (1993)

E. K. Yeh, John Newman, and C. J. Radke, "Equilibrium configurations of liquid droplets on solid surfaces under the influence of thin-film forces Part I: Thermodynamics," *Colloids and Surfaces A*. **156**, 137 (1999)

L. M. Hocking, "The spreading of drops with intermolecular forces," *Phys. Fluids*. **6(10)**, 3224 (1994)

D. Bhatt, J. Newman, and C. J. Radke, "Molecular Simulation of Disjoining-Pressure Isotherms for Free Liquid, Lennard-Jones Thin Films," *J. Phys. Chem. B.* **106(25)**, 6529 (2002)

I. Veretennikov, A. Indeikina, and H. Chang, "Front dynamics and fingering of a driven contact line," *J. Fluid Mech*. **373**, 81 (1998)

S. D. Taylor, J. Czarnecki, and J. Masliyah, "Disjoining Pressure Isotherms of Water-in-Bitumen Emulsion Films," *J. Colloid and Interface Sci.* **252**, 149 (2002)

A. Oron, S. H. Davis, S. G. Bankoff, "Long-scale evolution of thin liquid films," *Reviews of Modern Physics.* **69(3)**, July 1997, pp931-980.

H. Wong, D. Rumschitzki, C. Maldarelli, "Marangoni effects on the motion of an expanding or contracting bubble pinned at a submerged tube tip," *J.Fluid Mech.* **379**, 1999, pp279-302.

H. Wong, D. Rumschitzki, C. Maldarelli, “On the surfactant mass balance at a deforming fluid interface,” *Phys.Fluid.* **8**, 1996, pp3203-3204.

P. K. Kundu, *Fluid Mechanics*, Academic Press, Inc., San Diego, California, (1990)

J. S. Rowlinson, and B. Widom, *Molecular Theory of Capillarity*, Oxford University Press, New York, (1989)

C. A. Miller, and P. Neogi, *Interfacial Phenomena*, Marcel Dekker, Inc., New York and Basel, (1985)

X. Zhang, P. Neogi, and R. M. Ybarra, “Stable Drop Shapes under Disjoining Pressure I. A Hierachical Approach and Application,” *J. Colloid and Interface Sci*. **249**, 134 (2002).

X. Zhang and P. Neogi, “Stable Drop Shapes under Disjoining Pressure II. Multiplicity and Stability,” *J. Colloid and Interface Sci*. **249**, 141 (2002).

N. V. Churaev, V. D. Sobolev, and V. M. Starov, “Disjoining Pressure of Thin Nonfreezing Interlayers,” *J. Colloid and Interface Sci*. **247**, 80 (2002).

P. G. de Gennes, “Wetting: statics and dynamics,” *Rev. Mod. Phys.* **57(3)**, **Part I**, 827 (1985)

S. Kalliadasis, and H. Chang, “Apparent dynamic contact angle of an advancing gas-liquid meniscus,” *Phys. Fluids.* **6(1)**, 12 (1994)

APPENDIX A.
THE TOTAL INTERMOLECULAR POTENTIAL PHI PER UNIT VOLUME

The total intermolecular potential per unit volume is

$$\Phi = n_f(\Phi_{ff} + \Phi_{fs} + \Phi_{fg}), \tag{A.1}$$

where n_f is the number density of the liquid molecules, Φ_{ff} is the intermolecular potential between a liquid molecule M and the rest of the liquid wedge outside a sphere of radius D surrounding M, Φ_{fs} is the intermolecular potential between M and the semi-infinite solid substrate, and Φ_{fg} is that between M and the vapor (Fig. 2). A cylindrical coordinate system (r, θ, z) is defined as shown in Fig. 2 for a point N, with z perpendicular to x and y. In terms of these coordinates, the liquid molecule M is located at $(R, \gamma, 0)$. Thus, the distance MN between M and N can be found from

$$MN^2 = R^2 + r^2 + z^2 - 2rR\cos(\theta - \gamma). \tag{A.2}$$

This gives

$$\Phi_{fs} = \iiint_{V_s} n_s \phi_{fs} dV = \int_{\pi}^{2\pi} \int_0^{\infty} \int_{-\infty}^{\infty} \frac{-n_s \beta_{fs}}{MN^6} r dz dr d\theta, \tag{A.3}$$

where n_s is the number density of the solid molecules and ϕ_{fs} is the van der Walls potential in (3.1). Since the solid domain is unbounded in x, Φ_{fs} should be independent of x and should depend only on v_1, the height of M (Fig. 2).

We evaluate the integration in (A.3) in the following steps.

$$\int_{-\infty}^{\infty} \frac{dz}{[R^2 + r^2 + z^2 - 2rR\cos(\theta-\gamma)]^3} = \frac{3\pi}{8[R^2 + r^2 - 2rR\cos(\theta-\gamma)]^{5/2}}. \quad \text{A.4)}$$

Define $\omega = \theta - \gamma$, then

$$\int_0^{\infty} \frac{3\pi}{8[R^2 + r^2 - 2rR\cos(\theta-\gamma)]^{5/2}} rdr = \frac{\pi}{8(1-\cos(\theta-\gamma))^2 R^3}. \quad \text{(A.5)}$$

Define $G(\omega) = \csc^3\omega + \cot^3\omega + 3(\cot\omega)/2$, then

$$\int \frac{\pi}{8(1-\cos(\theta-\gamma))^2 R^3} d\theta = \frac{-\pi}{12R^3} G(\omega). \quad \text{(A.6)}$$

Then (A.3) gives

$$\Phi_{fs} = \frac{\pi n_s \beta_{fs}}{12R^3}\big(G(2\pi-\gamma) - G(\pi-\gamma)\big). \quad \text{(A.7)}$$

Simplification of (A.7) becomes

$$\Phi_{fs} = -\frac{\pi n_s \beta_{fs}}{6v_1^3}, \quad \text{(A.8)}$$

where

$$v_1 = R\sin\gamma. \quad \text{(A.9)}$$

The intermolecular potential from the vapor can be evaluated similarly.

$$\Phi_{fg} = \iiint_{V_g} n_g \phi_{fg} dV = \int_{\psi}^{\pi}\int_0^{\infty}\int_{-\infty}^{\infty} \frac{-n_g\beta_{fg}}{MN^6} rdzdrd\theta = \frac{-\pi n_g \beta_{fg}}{6}\left(\frac{a_1 - 1}{v_1^3} + \frac{a_2}{v_2^3}\right), \quad \text{(A.10)}$$

where $v_2 = R\sin(\psi-\gamma)$ is the normal distance of M from the wedge surface (Fig. 2), and

$$a_1 = \frac{1}{2} + \frac{3}{4}\cos\gamma - \frac{1}{4}\cos^3\gamma, \quad \text{(A.11)}$$

$$a_2 = \frac{1}{2} + \frac{3}{4}\cos(\psi - \gamma) - \frac{1}{4}\cos^3(\psi - \gamma). \tag{A.12}$$

To calculate Φ_{ff}, it is easier to find the total and the compliment, instead of direct integration. The intermolecular potential between M and an infinite body of liquid V_{-D} outside a sphere of radius D surrounding M is

$$\Phi_{-D} = \iiint_{V_{-D}} n_f \phi_{ff} dV = \int_D^\infty -\frac{n_f \beta_{ff}}{r^6}(4\pi r^2)dr = -\frac{4\pi n_f \beta_{ff}}{3D^3}. \tag{A.13}$$

If the vapor and solid regions are assumed to be filled with liquid, then the intermolecular potential between M and these regions is

$$\Phi_C = -\frac{\pi n_f \beta_{ff}}{6v_1^3} - \frac{\pi n_f \beta_{ff}}{6}\left(\frac{a_1 - 1}{v_1^3} + \frac{a_2}{v_2^3}\right), \tag{A.14}$$

where results for Φ_{fs} and Φ_{fg} have been used with $n_s\beta_{fs}$ and $n_g\beta_{fg}$ replaced by $n_f\beta_{ff}$. Thus,

$$\Phi_{ff} = \Phi_{-D} - \Phi_C = -\frac{4\pi n_f \beta_{ff}}{3D^3} + \frac{\pi n_f \beta_{ff}}{6}\left(\frac{a_1}{v_1^3} + \frac{a_2}{v_2^3}\right). \tag{A.15}$$

This solution is symmetric about the bisector of the wedge, as expected.

The total intermolecular potential per unit volume at point M in the liquid is

$$\Phi = n_f(\Phi_{ff} + \Phi_{fs} + \Phi_{fg}) = \frac{\pi n_f^2 \beta_{ff}}{6}\left(\frac{a_1(1-\rho) + \rho - \lambda}{v_1^3} + \frac{a_2(1-\rho)}{v_2^3}\right), \tag{A.16}$$

$$\lambda = \frac{n_s \beta_{fs}}{n_f \beta_{ff}}, \tag{A.17}$$

$$\rho = \frac{n_g \beta_{fg}}{n_f \beta_{ff}}, \tag{A.18}$$

where the potential has been increased by a constant value of $4\pi n_f^2 \beta_{ff} / 3D^3$. The potential Φ holds for arbitrary small wedge angle ψ.

APPENDIX B. THE INTERACTION POTENTIAL E PER UNIT AREA

From (3.5),

$$E = \int_0^h (\Phi - \Phi_\infty) dy . \tag{B.1}$$

The total intermolecular potential Φ per unit volume is a function of the position of point M. Thus, the height of M is $v_1 = y$, and the normal distance from the wedge surface is $v_2 = (h - y)\cos\psi$ (Fig. 2). Substitution of Φ in (A.16) gives

$$E = \frac{\pi n_f^2 \beta_{ff}}{6} \left(\int_D^h \frac{a_1(1-\rho) + \rho - \lambda}{y^3} dy + (1-\rho) \int_0^{h-D} \frac{(a_2 - 1)}{(h-y)^3 \cos^3\psi} dy \right), \tag{B.2}$$

where a cut-off has been applied to the first integral on the right side to avoid unbounded interaction at the liquid-solid interface. The singularity arises because the cut-off sphere surrounding M is assumed to contain only liquid molecules. If M is at the liquid-solid interface, it interacts with adjacent solid molecules resulting in an infinite interaction that cannot be prevented by the cut-off liquid sphere. Thus, an additional truncation is needed at the liquid-solid interface. A similar cut-off is also applied to the second integral at the liquid-vapor interface. As the position of M varies, the wedge angle ψ stays fixed, but the angle γ changes (Fig. 2). From geometry,

$$\cos\gamma = \frac{h}{\left[h^2 + h_x{}^2 y^2\right]^{1/2}}, \tag{B.3}$$

$$\cos(\psi-\gamma)=\left[1-\frac{h_x^2(h-y)^2}{(1+h_x^2)\left(h^2+h_x^2y^2\right)}\right]^{1/2}. \tag{B.4}$$

These expressions are substituted into a_1 and a_2:

$$\begin{aligned}\int_D^h \frac{a_1(1-\rho)+\rho-\lambda}{v_1^3}dy &= -\left(\frac{1}{h^2}-\frac{1}{D^2}\right)\left(\frac{1+\rho-2\lambda}{4}\right)\\ &\quad+\frac{1-\rho}{4}\left[\frac{h}{D^2\left(h^2+h_x^2D^2\right)^{1/2}}-\frac{1}{h^2\left(1+h_x^2\right)^{1/2}}\right],\end{aligned} \tag{B.5}$$

$$\begin{aligned}\int_0^{h-D}\frac{(a_2-1)}{v_2^3}dy &= \frac{h^3+h_x^4(h^2-D^2)(h-D)+h_x^2h^2(2h-D)}{4D^2h^2\left[h^2+h_x^2(D-h)^2\right]^{1/2}}\\ &\quad+\frac{(1+h_x^2)^{3/2}}{4}\left(\frac{1}{h^2}-\frac{1}{D^2}\right)-\frac{1+h_x^2}{4h^2},\end{aligned} \tag{B.6}$$

where $\cos\psi=\left(1+h_x{}^2\right)^{-1/2}$ has been invoked. The above results are exact.

In most applications, the slope of the liquid film is small, i.e., h_x <<1. Thus, (B.4) and (B.5) are expanded in the limit $h_x\to 0$:

$$E=-\frac{\pi n_f^2\beta_{ff}(1-\rho)}{64h^2}\left[\frac{16}{3}\left(\frac{1-\lambda}{1-\rho}\right)+h_x^4\right]+\frac{\pi n_f^2\beta_{ff}(1-\lambda)}{12D^2}\left[1+\frac{3(1-\rho)h_x^4}{8(1-\lambda)}\frac{D^4}{h^4}\right]. \tag{B.7}$$

The second term is constant in the limit $D/h\to 0$ and can be eliminated since E is a potential.

APPENDIX C.
ASYMPTOTIC SOLUTION OF THE FILM PROFILES FOR C=0

Equation (4.16)

$$H_{\varsigma\varsigma} - \left(\frac{1 - \varepsilon^2 H_\varsigma^4 + 2\varepsilon^2 H H_\varsigma^2 H_{\varsigma\varsigma}}{H^3} \right) = 0 , \tag{C.1a}$$

is subject to the symmetry condition at $\varsigma = 0$:

$$H = 1, \tag{C.1b}$$

$$H_\varsigma = 0 . \tag{C.1c}$$

In the limit $\varepsilon \to 0$,

$$H(\varsigma) = H_0(\varsigma) + \varepsilon^2 H_1(\varsigma) . \tag{C.2}$$

Substitution into (C.1a) yields

$$H_{0\varsigma\varsigma} - \frac{1}{H_0^3} + \varepsilon^2 \left(H_{1\varsigma\varsigma} + \frac{3H_1}{H_0^4} - \frac{-H_{0\varsigma}^4 + 2H_0 H_{0\varsigma}^2 H_{0\varsigma\varsigma}}{H_0^3} \right) = 0 . \tag{C.3a}$$

At $\varsigma = 0$,

$$H_0 = 1, \tag{C.3b}$$

$$H_1 = 0 , \tag{C.3c}$$

$$H_{0\varsigma} = H_{1\varsigma} = 0 . \tag{C.3d}$$

An analytic solution is found for H_0:

$$H_0 = \left(\varsigma^2 + 1 \right)^{1/2} . \tag{C.4}$$

As $\varsigma \to \infty$, $H_{0\varsigma} \to 1$. Thus, the leading-order solution captures the asymptotic value of the slope in (4.17).

The first-order expansion H_1 obeys

$$H_{1\varsigma\varsigma} + \frac{3H_1}{\left(\varsigma^2+1\right)^2} + \frac{\varsigma^2\left(\varsigma^2-2\right)}{\left(\varsigma^2+1\right)^{7/2}} = 0. \tag{C.5}$$

The corresponding boundary conditions are that at $\varsigma = 0$, $H_1 = 0$, $H_{1\varsigma} = 0$. An analytic solution exists:

$$H_1 = -\frac{\varsigma^2}{4(\varsigma^2+1)^{3/2}}\left(1 - \frac{(\varsigma^2+1)\tan^{-1}(\varsigma)}{\varsigma}\right). \tag{C.6}$$

As $\varsigma \to \infty$, $H_1 \to \pi/8$ and $H_{1\varsigma} \to 0$. Substitution (C.4) and (C.6) into (C.2) gives the perturbation solution for C=0:

$$H = H_0 + \varepsilon^2 H_1 = \sqrt{\varsigma^2+1} - \frac{\varepsilon^2\varsigma^2}{4(\varsigma^2+1)^{3/2}}\left(1 - \frac{(\varsigma^2+1)\tan^{-1}(\varsigma)}{\varsigma}\right). \tag{C.7}$$

APPENDIX D.
DROP PROFILES BY MATCHED ASYMPTOTIC EXPANSIONS

The dimensionless equation governing the profile of a drop with positive disjoining pressure is

$$H_{XX} + \varepsilon\left(\frac{1 - H_X^4 + 2HH_X^2H_{XX}}{H^3}\right) = C. \tag{D.1}$$

Since C is unknown, the symmetric condition at $X = 0$ ($H = 1,\ H_X = 0$) cannot solve the problem with $\varepsilon = 0$, because the boundary condition at the contact line is eliminated by setting $\varepsilon = 0$. Thus, $\varepsilon \to 0$ is singular and an inner region exists near the contact line. In the inner region, the capillary pressure balances the disjoining pressure to yield $\delta H \sim \delta X \sim \varepsilon^{1/2}$, where δH and δX are the length scales of H and X.

In the inner region, a set of variables is defined:

$$\eta = \frac{H}{\varepsilon^{1/2}}, \tag{D.2}$$

$$\xi = \frac{X - X_0}{\varepsilon^{1/2}}, \tag{D.3}$$

where $X_0 = X_0(\varepsilon)$ is the position of the contact line. Equation (D.1) becomes

$$\eta_{\xi\xi} + \frac{1 - \eta_\xi^4 + 2\eta\eta_\xi^2\eta_{\xi\xi}}{\eta^3} = \varepsilon^{1/2}C. \tag{D.4}$$

At the contact line, $\xi \to 0, \eta \to 0$. This is the only boundary condition in the inner region. Other boundary conditions must come form matching.

The variables are expanded in series of $\varepsilon^{1/2}$:

$$\eta = \eta_0 + \varepsilon^{1/2}\eta_1 + \varepsilon\eta_2 + \cdots, \tag{D.5a}$$

$$C = C_0 + \varepsilon^{1/2}C_1 + \varepsilon C_2 + \cdots, \tag{D.5b}$$

$$X_0 = X_{00} + \varepsilon^{1/2}X_{01} + \varepsilon X_{02} + \cdots. \tag{D.5c}$$

Substitution into (D.4) yields

$$\begin{aligned}&\eta_{0\xi\xi} + \frac{1-\eta_{0\xi}^4 + 2\eta_0\eta_{0\xi}^2\eta_{0\xi\xi}}{\eta_0^3} + \varepsilon^{1/2}\eta_{1\xi\xi} + \varepsilon^{1/2}\,\frac{3\eta_1\left(1-\eta_{0\xi}^4 + 2\eta_0\eta_{0\xi}^2\eta_{0\xi\xi}\right)}{\eta_0^4}\\ &+\varepsilon^{1/2}\left[\frac{-4\eta_{0\xi}^3\eta_{1\xi} + 2\eta_0\eta_{0\xi}^2\eta_{1\xi\xi} + (4\eta_0\eta_{0\xi}\eta_{1\xi} + 2\eta_1\eta_{0\xi}^2)\eta_{0\xi\xi}}{\eta_0^3}\right] = \varepsilon^{1/2}C_0.\end{aligned} \tag{D.6}$$

To leading order,

$$\eta_{0\xi\xi} + \frac{1-\eta_{0\xi}^4 + 2\eta_0\eta_{0\xi}^2\eta_{0\xi\xi}}{\eta_0^3} = 0. \tag{D.7}$$

This equation is the same as (4.5) with $C = 0$ and $\varepsilon = 1$. From §4.1, the only solution that contacts the substrate is

$$\eta_0 = -\xi. \tag{D.8}$$

This is to be matched to the outer solution

The outer variables also need to be expanded in series of $\varepsilon^{1/2}$:

$$H = H_0 + \varepsilon^{1/2}H_1 + \varepsilon H_2 + \cdots, \tag{D.9}$$

Substitution into (D.1) leads to

$$H_{0XX} + \varepsilon^{1/2}H_{1XX} + \varepsilon\left(\frac{1-H_{0X}^4 + 2H_0H_{0X}^2H_{0XX}}{H_0^3}\right) = C_0 + \varepsilon^{1/2}C_1 + \varepsilon C_2 \tag{D.10a}$$

At $X = 0$,

$$H_0 + \varepsilon^{1/2}H_1 + \varepsilon H_2 = 1, \tag{D.10b}$$

$$H_{0X} + \varepsilon^{1/2} H_{1X} + \varepsilon H_{2X} = 0 . \tag{D.10c}$$

The leading-order solution is

$$H_0 = \frac{C_0}{2} X^2 + 1. \tag{D.11}$$

The leading pressure jump C_0 must be found by matching.

Inner and outer expansions are matched by taking the outer limit of the inner expansions and the inner limit of the outer expansions:

$$\lim_{X \to X_0} H = \lim_{\xi \to -\infty} \varepsilon^{1/2} \eta . \tag{D.12}$$

In the limit $X \to X_0 = X_{00}$,

$$H_0 \to \frac{C_0}{2}(X - X_0)^2 + C_0 X_{00}(X - X_0) + \frac{C_0}{2} X_{00}^2 + 1. \tag{D.13}$$

In the limit $\xi \to -\infty$,

$$\varepsilon^{1/2} \eta \to -(X - X_0). \tag{D.14}$$

Matching (D.13) and (D.14) yields

$$X_{00} = 2, \tag{D.15}$$

$$C_0 = -\frac{1}{2}, \tag{D.16}$$

Thus, the leading order composite solution is

$$H_c = H_0 + \varepsilon^{\frac{1}{2}} \eta_0 - \eta_{match} = -\frac{1}{4} X^2 + 1. \tag{D.17}$$

The first-order inner film height obeys

$$\eta_{1\xi\xi} - \frac{4}{\xi(2 + \xi^2)} \eta_{1\xi} = \frac{-\xi^2}{2(\xi^2 + 2)}. \tag{D.18}$$

At $\xi = 0$,

$$\eta_1 = 0, \tag{D.19}$$

An analytical solution is found:

$$\eta_1 = -\frac{1}{4}\xi^2 + \frac{1}{2}\ln\left(\frac{\xi^2+2}{2}\right) + K_1\left(\xi - \sqrt{2}\arctan\left(\frac{\xi}{\sqrt{2}}\right)\right), \tag{D.20}$$

where K_1 is an integration constant to be determined by matching.

The first-order outer region solution is

$$H_1 = \frac{C_1}{2}X^2, \tag{D.21}$$

where C_1 needs to be found by matching.

The matching principle (D.12) is invoked again. In the limit $X \to X_0 = X_{00} + \varepsilon^{1/2}X_{01}$,

$$\begin{aligned} H_0 + \varepsilon^{1/2}H_1 \to & -\frac{1}{4}(X - X_0)^2 - (X - X_0) \\ & + \varepsilon^{1/2}\left(\frac{1}{2}C_1(X - X_0)^2 + (2C_1 - \frac{1}{2}X_{01})(X - X_0) + 2C_1 - X_{01}\right). \end{aligned} \tag{D.22}$$

In the limit $\xi \to -\infty$,

$$\varepsilon^{1/2}\eta_0 + \varepsilon\eta_1 \to -\frac{1}{4}(X - X_0)^2 - (X - X_0) + \varepsilon^{1/2}K_1(X - X_0). \tag{D.23}$$

Matching (D.22) and (D.23) yields

$$X_{01} = 2C_1, \tag{D.24}$$

$$K_1 = C_1. \tag{D.25}$$

APPENDIX E. PROGRAMS

E.1. Equilibrium film profiles for C=0 with symmetric central condition (equiC0.for)

```
C---------- THIS IS A PROGRAM TO CACULATE THE EQUILIBRIUM    ---------
C ---------    SHAPE WITH C=0 AND SYMMETRIC CENTRAL CONDITION    --
          EXTERNAL F
          DIMENSION Y(2),D(2),B(2),C(2),G(2)
          DOUBLE PRECISION Y,D,T,B,C,G,E,DX
          COMMON /ONE/ E
          OPEN(15,FILE='EQUIC0.TXT',STATUS='UNKNOWN')
          E=1D-2
          DX=5.0D-2
          EPS=1.0D-7
          T=0.0D0
C-------------  Y(1) IS H0, Y(2) IS HX    ----------------------------
          Y(1)=1.0D0
          Y(2)=0.0D0
          M=2
          WRITE(15,*) E
          DO 10 I=1,100
              CALL RKT(T,DX,Y,M,F,EPS,D,B,C,G)
              T=T+DX
              WRITE(15,50) T,Y(1)
10        CONTINUE
50        FORMAT(2D25.16)
          CLOSE(15)
          END

          SUBROUTINE F(T,Y,M,D)
          DIMENSION Y(M),D(M)
          DOUBLE PRECISION Y,D,T,E
          COMMON /ONE/ E
          D(1)=Y(2)
          D(2)=(1-E**2D0*Y(2)**4)/(Y(1)**3-2D0*E**2D0*Y(1)*Y(2)**2D0)
          RETURN
          END
          SUBROUTINE RKT(T,H,Y,M,F,EPS,D,B,C,G)
```

```
      DIMENSION Y(M),D(M),A(4),B(M),C(M),G(M)
      DOUBLE PRECISION Y,D,A,B,C,G,T,H,X,HH,TT
      HH=H
      N=1
      P=1.0D0+EPS
      X=T
      DO 5 I=1,M
5     C(I)=Y(I)
10    IF(P.GE.EPS) THEN
          A(1)=HH/2.0D0
          A(2)=A(1)
          A(3)=HH
          A(4)=HH
          DO 20 I=1,M
              G(I)=Y(I)
              Y(I)=C(I)
20        CONTINUE
          DT=H/N
          T=X
          DO 100 J=1,N
              CALL F(T,Y,M,D)
              DO 30 I=1,M
30                B(I)=Y(I)
              DO 50 K=1,3
                  DO 40 I=1,M
                      Y(I)=Y(I)+A(K)*D(I)
                      B(I)=B(I)+A(K+1)*D(I)/3.0D0
40                CONTINUE
                  TT=T+A(K)
                  CALL F(TT,Y,M,D)
50            CONTINUE
              DO 60 I=1,M
60                Y(I)=B(I)+HH*D(I)/6.0D0
              T=T+DT
100       CONTINUE
          P=0.0D0
          IF(Y(1).LE.0.0D0) THEN
              GOTO 110
          ELSE
              Q=ABS(Y(1)-G(1))
```

```
            IF(Q.GT.P) P=Q
          END IF
            HH=HH/2.0D0
          N=N+N
          GOTO 10
        END IF
110     CONTINUE
        T=X
        RETURN
        END
```

E.2. Equilibrium drop profiles and half drop volume with positive disjoining pressure (equiCnegative.for)

```
C----- THIS IS A PROGRAM TO CACULATE THE EQUILIBRIUM    ------
C -----DROP SHAPE WITH C<0 AND SYMMETRIC CENTRAL CONDITION
C------    THE SUBROUTINE RKT IS THE SAME IN APPENDIX D.1.
          EXTERNAL F
          DIMENSION Y(2),D(2),B(2),C(2),G(2),XX(0:100),HH(0:100)
          DOUBLE PRECISION Y,D,T,DX,B,C,G,E,TT1,TT2,HH1,HH2
          COMMON /ONE/ E
          OPEN(15,FILE='DROP_EQU.TXT',STATUS='UNKNOWN')
          OPEN(16,FILE='X0_AND_V.TXT',STATUS='UNKNOWN')
          E=1D-2
          DX=5.0D-2
          EPS=1.0D-7
          T=0.0D0
          XX(0)=T
C-------------  Y(1) IS H0, Y(2) IS HX    ----------------------------
          Y(1)=1.0D0
          Y(2)=0.0D0
          M=2
          HH(0)=Y(1)
          DO 10 I=1,100
              CALL RKT(T,DX,Y,M,F,EPS,D,B,C,G,HNEW)
               T=T+DX
               IF((Y(1).GT.0.0)) THEN
                   TT1=T
                   HH1=Y(1)
                   XX(I)=T
                   HH(I)=Y(1)
                   WRITE(15,50) T,Y(1)
                   GO TO 10
               ELSE
                   TT2=T
                   HH2=Y(1)
                   X0=TT1+(TT2-TT1)/(HH1-HH2)*HH1
                   Y(1)=0D0
                   XX(I)=T
                   HH(I)=Y(1)
                   WRITE(15,50) X0,Y(1)
```

```
                WRITE(16,60) X0
                GO TO 100
            END IF
10      CONTINUE
100     CONTINUE
        V=0D0
        DO 70 J=0,I-1
        V=V+(HH(J)+HH(J+1))*(XX(J+1)-XX(J))/2D0
70      CONTINUE
        WRITE(16,60) V
50      FORMAT(2D25.16)
60      FORMAT(D25.16)
        CLOSE(15)
        END

        SUBROUTINE F(T,Y,M,D)
        DIMENSION Y(M),D(M)
        DOUBLE PRECISION Y,D,T,C,E,ALPHA
        COMMON /ONE/ E
        C=-(E+1.0D0)/2.0D0
        D(1)=Y(2)
        D(2)=(C*Y(1)**3-E*(1D0-Y(2)**4))/(Y(1)**3+2D0*E*Y(1)*Y(2)**2D0)
        RETURN
        END
```

E.3. Half of drop width X_0

(X0maple.mws)

```
> restart;
> e:=epsilon;
```

$$e := \varepsilon$$

```
>
eqt:=(1/(2*e)*(-H^2+sqrt(H^4-4*e*(1+e)*H^3+4*e*H^2+4*e^2))
)^(-1/2);
```

$$eqt := \frac{\sqrt{2}}{\sqrt{\frac{-H^2+\sqrt{H^4-4\,\varepsilon\,H^3-4\,\varepsilon^2\,H^3+4\,\varepsilon\,H^2+4\,\varepsilon^2}}{\varepsilon}}}$$

```
> epsilon:=2e-4;X0:=(int(eqt,H=0..1.0));
```

$$\varepsilon := .0002$$

$$X0 := 1.998746528$$

```
> epsilon:=8e-4;X0:=(int(eqt,H=0..1.0));
```

$$\varepsilon := .0008$$

$$X0 := 1.995567103$$

```
> epsilon:=1e-3;X0:=(int(eqt,H=0..1.0));
```

$$\varepsilon := .001$$

$$X0 := 1.994578507$$

```
> epsilon:=2e-3;X0:=(int(eqt,H=0..1.0));
```

$$\varepsilon := .002$$

$$X0 := 1.989914886$$

```
> epsilon:=5e-3;X0:=(int(eqt,H=0..1.0));
```

$$\varepsilon := .005$$

$$X0 := 1.977413166$$

```
> epsilon:=1e-2;X0:=(int(eqt,H=0..1.0));
```

$$\varepsilon := .01$$

$$X0 := 1.959077708$$

```
> epsilon:=2e-2;X0:=(int(eqt,H=0..1.0));
```

$$\varepsilon := .02$$

$$X0 := 1.927356193$$

```
> epsilon:=3e-2;X0:=(int(eqt,H=0..1.0));
```

$$\varepsilon := .03$$

$$X0 := 1.899721423$$

```
> epsilon:=4e-2;X0:=(int(eqt,H=0..1.0));
```

$$\varepsilon := .04$$

$$X0 := 1.874925979$$

```
> epsilon:=5e-2;X0:=(int(eqt,H=0..1.0));
```

$$\varepsilon := .05$$

$$X0 := 1.852327582$$

```
> epsilon:=6e-2;X0:=(int(eqt,H=0..1.0));
```

$$\varepsilon := .06$$

$$X0 := 1.831522593$$

```
> epsilon:=7e-2;X0:=(int(eqt,H=0..1.0));
```

$$\varepsilon := .07$$

$$X0 := 1.812229549$$

```
> epsilon:=8e-2;X0:=(int(eqt,H=0..1.0));
```

$$\varepsilon := .08$$

$$X0 := 1.794239156$$

```
> epsilon:=9e-2;X0:=(int(eqt,H=0..1.0));
```

$$\varepsilon := .09$$

$$X0 := 1.777388845$$

```
> epsilon:=1e-1;X0:=(int(eqt,H=0..1.0));
```

$$\varepsilon := .1$$

$$X0 := 1.761548314$$

```
> epsilon:=1e0;X0:=(int(eqt,H=0..1.0));
```

$$\varepsilon := 1.$$

$$X0 := 1.346387357$$

E.4. A uniform film growing to a meniscus
(uniformgrow.for)

```
C-----------   UNIFORM FILM GROWS TO A MENISCUS     ---------
C------   THE SUBROUTINE RKT IS THE SAME IN APPENDIX D.1.   ----------
          EXTERNAL F
          DIMENSION Y(2),D(2),B(2),C(2),G(2)
          DOUBLE PRECISION Y,D,T,DX,B,C,G,E,AM
          COMMON /ONE/ E
          OPEN(15,FILE='UNIFORMTOMENISCUS.TXT',STATUS='UNKNOWN')
          N=1000
          AM=1.0D-3
          E=1D-2
          DX=5.0D-2
          EPS=1.0D-7
          T=0.0D0
C-------------  Y(1) IS H0, Y(2) IS HX   ----------------------------
          Y(1)=1D0+AM
          Y(2)=SQRT(3D0)*AM
          M=2
          DO 10 I=1,N
              CALL RKT(T,DX,Y,M,F,EPS,D,B,C,G)
              T=T+DX
              WRITE(15,50) T,Y(1)
10        CONTINUE
50        FORMAT(2D25.16)
          CLOSE(15)
          END

          SUBROUTINE F(T,Y,M,D)
          DIMENSION Y(M),D(M)
          DOUBLE PRECISION Y,D,T,E
          COMMON /ONE/ E
          D(1)=Y(2)
          D(2)=(Y(1)**3D0-1+E**2D0*Y(2)**4)/(Y(1)**3+2D0*E**2D0*Y(1)*Y(2)**2
      D0)
          RETURN
          END
```

E.5. A wedge film growing to a meniscus (contactlinegrow.for)

```
C-----------   CONTACT LINE GROWS TO A MENISCUS   ---------------------
C------  THE SUBROUTINE RKT IS THE SAME IN APPENDIX D.1.   ----------
      EXTERNAL F
      DIMENSION Y(2),D(2),B(2),C(2),G(2)
      DOUBLE PRECISION Y,D,T,DX,B,C,G,E,DELTAX
      COMMON /ONE/ E
      OPEN(15,FILE='CONT_TO_MENI.TXT',STATUS='UNKNOWN')
      N=100
      E=1D-2
      DELTAX=1D-2
      DX=5.0D-2
      EPS=1.0D-7
      T=DELTAX
C-------------  Y(1) IS H0, Y(2) IS HX   ----------------------------
      Y(1)=DELTAX+1D0/(8D0*E)*(DELTAX**4D0)
      Y(2)=1+1D0/(2D0*E)*(DELTAX**3D0)
      M=2
      DO 10 I=1,N
          CALL RKT(T,DX,Y,M,F,EPS,D,B,C,G)
           T=T+DX
           WRITE(15,50) T,Y(1)
10    CONTINUE
50    FORMAT(2D25.16)
      CLOSE(15)
      END

      SUBROUTINE F(T,Y,M,D)
      DIMENSION Y(M),D(M)
      DOUBLE PRECISION Y,D,T,E
      COMMON /ONE/ E
      D(1)=Y(2)
      D(2)=(Y(1)**3-E*(1D0-Y(2)**4))/(Y(1)**3+2D0*E*Y(1)*Y(2)**2D0)
      RETURN
      END
```

E.6. Evolution of a step thin film with fixed contact line (evolution.for)

```
C------------     EVOLUTION OF A STEP THIN FILM     --------------------------
C------------     NEWTON-RAPHSON METHOD             --------------------------
          USE PORTLIB
          PARAMETER(N=2000)
          DIMENSION H(0:N),HN(0:N),X(0:N),H0(0:N),HH(0:10,0:N),SSUM(0:N)
          DIMENSION F(N),M(N,N),HPRO(N,0:N),THPRO(N)
          DIMENSION SURFACE(0:N),TSURFACE(0:N)
          DOUBLE PRECISION XLENGTH,DX,DT,EPSL,H,HN,X,HH,SSUM,F,M
          DOUBLE PRECISION ERROR,ERR,EPS,TIMERUN
          DOUBLE PRECISION HPRO,THPRO,SURFACE,TSURFACE,SUR
          CHARACTER(8) WHATIMEISIT,WHATDATE
          OPEN(10,FILE='RUN_TIME.TXT',STATUS='UNKNOWN')
          OPEN(11,FILE='ORIGINAL.TXT',STATUS='UNKNOWN')
          OPEN(15,FILE='SURFACE.TXT',STATUS='UNKNOWN')
          OPEN(17,FILE='IT1.TXT',STATUS='UNKNOWN')
          OPEN(18,FILE='IT2.TXT',STATUS='UNKNOWN')
          OPEN(19,FILE='IT3.TXT',STATUS='UNKNOWN')
          OPEN(20,FILE='IT4.TXT',STATUS='UNKNOWN')
C--------------- RECORD THE RUN TIME FOR PROGRAM    --------------
          WHATIMEISIT = CLOCK()
          WHATDATE = DATE()
          WRITE(10,*) 'PROGRAM BEGIN AT H:M:S = ',WHATIMEISIT
          WRITE(10,*) 'BEGIN DATE IS M/D/Y = ', WHATDATE
C------------       INITIAL PARAMETERS FOR PROGRAM    ------------------
          IHSTEP=10
          IHPRINT=1
          ITIMESTEP=10
          NT=100
          NX=200
          DT=1D-3
          EPSL=1D-2
          XLENGTH=25.0D0
          DX=XLENGTH/DBLE(NX)
          IX=INT(XLENGTH)
          EPS=1.0D-10
C----------------------     SET ORIGINAL SHAPE    --------------------------
          DO 10 I=0,NX/IX
```

```
            H(I)=DX*DBLE(I)
            X(I)=DX*DBLE(I)
10      CONTINUE
        DO 20 I=NX/IX+1,NX
            H(I)=1.0D0
            X(I)=DX*DBLE(I)
20      CONTINUE
C----------------------   END OF SETTIN INITIAL SHAPE   ------------
        WRITE(11,998) (X(I),H(I),I=0,NX)
        CALL SURFACE1(SUR,NX,H,DX,N)
        TIMESURFACE(0)=0D0
        SURFACE(0)=SUR
        DO 40 I=0,NX
            HN(I)=H(I)
            HH(0,I)=H(I)
40      CONTINUE
C ------------------   TIME MARCHING   ----------------------------------
        IFORHPROCESS=0
        IOFTIME=0
        DO WHILE(IOFTIME.LT.NT)
            IOFTIME=IOFTIME+1
            TIMERUN=DBLE(IOFTIME)*DT
            ERROR=1.0D0
C----------   IT IS THE ITERATION STEP NUMBER -------------------------------
            IT=0
            DO WHILE (ERROR.GE.EPS)
                ERROR=0D0
                IT=IT+1
                IF (IT.LE.10) THEN
                    CALL INPUT(H,HN,EPSL,DT,DX,F,M,NX,N)
                    CALL INVERSE(M,NX-1,N)
                    DO 120 I=1,NX-1
                        SSUM(I)=0D0
                        DO 130 J=1,NX-1
                            SSUM(I)=SSUM(I)+M(I,J)*F(J)
130                     CONTINUE
                        HH(IT,I)=HH(IT-1,I)-SSUM(I)
                        H(I)=HH(IT,I)
                        ERR=DABS(SSUM(I))
                        IF(ERR.GE.ERROR) THEN
```

```
                        ERROR=ERR
                    END IF
120                 CONTINUE
                    H(NX)=H(NX-1)
                ELSE
                    WRITE(*,*) 'ITERATION FAILED'
                    GOTO 6
                END IF
            END DO
            CALL SURFACE1(SUR,NX,H,DX,N)
            TIMESURFACE(IOFTIME)=TIMERUN
            SURFACE(IOFTIME)=SUR
            IF((SURFACE(IOFTIME)-SURFACE(0)).GT.0) THEN
                GOTO 6
            ELSE
            ENDIF
C---------  BEGIN TO PRINT OUT      ------------------------------------
C---------  SAVE FILM SHAPE PER IHSTEP   -------------------------
            I=MOD(IOFTIME,IHSTEP)
            IF(I.EQ.0) THEN
                IFORHPROCESS=IFORHPROCESS+1
                THPRO(IFORHPROCESS)=TIMERUN
                DO 165 I=0,NX
                    HPRO(IFORHPROCESS,I)=H(I)
165             CONTINUE
C----------------  PRINT OUT HPROCESS PER IHPRINT   ------------
                II=MOD(IFORHPROCESS,IHPRINT)
                IF(II.EQ.0) THEN
                    JJ=IFORHPROCESS/IHPRINT
                    WRITE(JJ+16,997) (THPRO(JJ))
                    WRITE(JJ+16,998) (X(I),HPRO(JJ,I),I=0,NX)
                END IF
            END IF
            DO 170 I=0,NX
                HN(I)=H(I)
                HH(0,I)=H(I)
170         CONTINUE
        END DO
6       CONTINUE
        WRITE(15,998) (TSURFACE(I),SURFACE(I),I=0,IOFTIME-1)
```

```
      IOFTIMEFINISH=IOFTIME
      WRITE(10,*) 'IOFTIME FINISH=',IOFTIMEFINISH
      WHATIMEISIT = CLOCK()
      WHATDATE = DATE()
      WRITE(10,*)
      WRITE(10,*) 'PROGRAM END AT H:M:S = ',WHATIMEISIT
      WRITE(10,*) 'END DATE IS MON/DAY/YEAR    ', WHATDATE
997   FORMAT(D25.16)
998   FORMAT(2D25.16)
      CLOSE(20)
      CLOSE(19)
      CLOSE(18)
      CLOSE(17)
      CLOSE(15)
      CLOSE(11)
      CLOSE(10)
      END


C------------     SUBROUTINE FOR CHECKING SURFACE    --------------------
      SUBROUTINE SURFACE1(SUR,NX,H,DX,N)
      DOUBLE PRECISION SUR,DX,H(0:N),HX(0:N),TEMP(0:N)
      SUR=0D0
      HX(0)=1D0
      HX(NX)=0D0
      DO 10 I=1,NX-1
            HX(I)=(H(I+1)-H(I-1))/(2D0*DX)
10    CONTINUE
      DO 20 I=0,NX
            TEMP(I)=SQRT(1D0+HX(I)**2D0)
20    CONTINUE
      DO 30 I=1,NX-1
            SUR=SUR+TEMP(I)
30    CONTINUE
      SUR=(SUR+0.5D0*(TEMP(0)+TEMP(NX)))*DX
      END

C-------    SUBROUTINE FOR INPUTING MATRIX F AND M
C------   BC:     AT X=0, H=0, HXX=0 , AT X=N, HX=0, HXX=0    ----------
      SUBROUTINE INPUT(H,HN,BETA,DT,DX,F,M,NX,N)
```

```
      DIMENSION H(0:N),HN(0:N)
      DIMENSION A(N),B(N),C(N),D(N),E(N),F(N),M(N,N)
      DIMENSION AP(N),BWW(N),BW(N),BP(N),BE(N),BEE(N)
      DIMENSION CWW(N),CW(N),CP(N),CE(N),CEE(N),DW(N)
      DIMENSION DP(N),DE(N),EE(N),EW(N),MWW(N),MW(N),MP(N)
      DIMENSION ME(N),MEE(N)
      DIMENSION BB(N),CC(N),DD(N),HX(N),HXX(N),HXXX(N),HXXXX(N)
      DOUBLE PRECISION DX,DT,BETA,H,HN,A,B,C,D,E,F,M,
      DOUBLE PRECISION AP,BWW,BW,BP,BE,BEE, CWW,CW,CP,CE,CEE
      DOUBLE PRECISION,DW,DP,DE,EE,EW,MWW,MW,MP,ME,MEE
      DOUBLE PRECISION BB,CC,DD,HM1,HNP1,HX,HXX,HXXX,HXXXX
      HM1=-H(1)
      HNP1=H(NX-1)
      H(NX)=H(NX-1)
      DO 10 I=1,NX-1
          HX(I)=(H(I+1)-H(I-1))/(2D0*DX)
          HXX(I)=(H(I+1)-2D0*H(I)+H(I-1))/(DX**2D0)
10    CONTINUE
      HXXX(1)=(H(3)-2D0*H(2)-HM1)/(2D0*DX**3D0)
      HXXXX(1)=(H(3)-4D0*H(2)+6D0*H(1)+HM1)/(DX**4D0)
      DO 20 I=2,NX-2
          HXXX(I)=(H(I+2)-2D0*H(I+1)+2D0*H(I-1)-H(I-2))/(2D0*DX**3D0)
          HXXXX(I)=(H(I+2)-4D0*H(I+1)+6D0*H(I)-4D0*H(I-1)+H(I-2))
     #            /(DX**4D0)
20    CONTINUE
      HXXX(NX-1)=(H(NX-1)-2D0*H(NX)+2D0*H(NX-2)
     #           -H(NX-3))/(2D0*DX**3D0)
      HXXXX(NX-1)=(H(NX-1)-4D0*H(NX)+6D0*H(NX-1)
     #            -4D0*H(NX-2)+H(NX-3))/(DX**4D0)
      DO 30 I=1,NX-1
          BB(I)=H(I)**3D0/3D0*(H(I)**2D0+2D0*BETA*HX(I)**2D0)/DX**4D0
          CC(I)=H(I)**2D0*(H(I)**2D0*HX(I)-2D0*BETA*HX(I)**3D0
     #           +4D0*BETA*H(I)*HX(I)*HXX(I))/(2*DX**3D0)
          DD(I)=BETA*(-20D0/3D0*H(I)**2D0*HX(I)**2D0*HXX(I)
     #          +4D0/3D0*H(I)**3D0*HXX(I)**2D0+5D0*H(I)*HX(I)**4D0-H(I))
          A(I)=H(I)**2D0/DT*(H(I)-HN(I))
          B(I)=BB(I)*HXXXX(I)*DX**4D0
          C(I)=CC(I)*HXXX(I)*(2D0*DX**3D0)
          D(I)=DD(I)*HXX(I)
          E(I)=BETA*HX(I)**2D0*(1D0-HX(I)**4D0)
```

```
          F(I)=A(I)+B(I)+C(I)+D(I)+E(I)
30      CONTINUE
        DO 60 I=1,NX-1
          AP(I)=H(I)/DT*(3.0D0*H(I)-2.0D0*HN(I))
60      CONTINUE
        DO 70 I=2,NX-2
          BWW(I)=BB(I)
          BW(I)=-4D0*BB(I)-2D0/3D0*HXXXX(I)*BETA*H(I)**3D0*HX(I)/DX
          BP(I)=6D0*BB(I)+1D0/3D0*HXXXX(I)*(5D0*H(I)**4D0+6D0*BETA*
     #          HX(I)**2D0*H(I)**2D0)
          BE(I)=-4D0*BB(I)+2D0/3D0*HXXXX(I)*BETA*H(I)**3D0*HX(I)/DX
          BEE(I)=BB(I)
          CWW(I)=-CC(I)
          CW(I)=2D0*CC(I)+H(I)**2D0*HXXX(I)*(-H(I)**2D0/(2D0*DX)
     #       +3*BETA*HX(I)**2D0/DX-2*BETA*H(I)*HXX(I)/DX+4*BETA*H(I)
     #       *HX(I)/DX**2D0)
          CP(I)=HXXX(I)*(4D0*H(I)**3D0*HX(I)+12D0*BETA*HX(I)*HXX(I)
     #       *H(I)**2D0-8D0*BETA*H(I)**3D0*HX(I)/DX**2D0
     #       -4D0*BETA*H(I)*HX(I)**3D0)
          CE(I)=-2D0*CC(I)+H(I)**2D0*HXXX(I)*(H(I)**2D0/(2D0*DX)
     #       -3*BETA*HX(I)**2D0/DX+2*BETA*H(I)*HXX(I)/DX+4*BETA*H(I)
     #       *HX(I)/DX**2D0)
          CEE(I)=CC(I)
70      CONTINUE
        DO 80 I=1,NX-1
          DW(I)=DD(I)/DX**2D0+BETA*HXX(I)*(-2D1/3D0*H(I)**2D0*HX(I)*
     #       (-HXX(I)/DX+HX(I)/DX**2D0)+8D0/3D0*H(I)**3D0*HXX(I)
     #        /DX**2D0-1D1*H(I)*HX(I)**3D0/DX)
          DP(I)=-2D0*DD(I)/DX**2D0+BETA*HXX(I)*(-4D1/3D0*HX(I)**2D0
     #        *H(I)* (HXX(I)-H(I)/DX**2D0)+4D0*H(I)**2D0*HXX(I)**2D0
     #        -1.6D1/3D0*H(I)**3*HXX(I)/DX**2D0+5D0*HX(I)**4D0-1D0)
          DE(I)=DD(I)/DX**2D0+BETA*HXX(I)*(-2D1/3D0*H(I)**2D0*HX(I)*
     #       (HXX(I)/DX+HX(I)/DX**2D0)+8D0/3D0*H(I)**3D0*HXX(I)
     #        /DX**2D0+1D1*H(I)*HX(I)**3D0/DX)
          EW(I)=-BETA*(HX(I)*(1D0-HX(I)**4D0)/DX-2D0*HX(I)**5D0/DX)
          EE(I)=-EW(I)
80      CONTINUE
        BWW(1)=0D0
        BW(1)=0D0
        BP(1)=5D0*BB(1)+1D0/3D0*HXXXX(1)*(5D0*H(1)**4D0+6D0*BETA*
```

```
#            HX(1)**2D0*H(1)**2D0)
  BE(1)=-4D0*BB(1)+1D0/3D0*HXXXX(1)*BETA*H(1)**
#           3D0*H(2)/DX**2D0
  BEE(1)=BB(1)
  CWW(1)=0D0
  CW(1)=0D0
  CP(1)=CC(1)+HXXX(1)*(4D0*H(1)**3D0*HX(1)+12D0*BETA
#         *HX(1)*HXX(1)*H(1)**2D0-8D0*BETA*H(1)**3D0*HX(1)/DX**2D0
#         -4D0*BETA*H(1)*HX(1)**3D0)
  CE(1)=-2D0*CC(1)+H(1)**2D0*HXXX(1)*(H(1)**2D0/(2D0*DX)
#         -3*BETA*HX(1)**2D0/DX+2*BETA*H(1)*HXX(1)/DX
#         +4*BETA*H(1)*HX(1)/DX**2D0)
  CEE(1)=CC(1)
  BE(NX-2)=BE(NX-2)+BB(NX-2)
  CE(NX-2)=CE(NX-2)+CC(NX-2)
  BEE(NX-1)=0D0
  BE(NX-1)=0D0
  BP(NX-1)=3D0*BB(NX-1)+1D0/3D0*HXXXX(NX-1)*(5D0*H(NX-1)**4D0
#             +6D0*BETA*HX(NX-1)**2D0*H(NX-1)**2D0
#             +2D0*BETA*HX(NX-1)*H(NX-1)**3D0/DX)
  BW(NX-1)=-4D0*BB(NX-1)-2D0/3D0*HXXXX(NX-1)*BETA
#              *H(NX-1)**3D0*HX(NX-1)/DX
  BWW(NX-1)=BB(NX-1)
  CEE(NX-1)=0D0
  CE(NX-1)=0D0
  CP(NX-1)=-CC(NX-1)+HXXX(NX-1)*(H(NX-1)**3D0*(4D0*HX(NX-1)
#      +H(NX-1)/(2D0*DX))-3D0*BETA*(HX(NX-1)*H(NX-1))**2D0/DX
#      -4D0*BETA*H(NX-1)*HX(NX-1)**3D0+4D0*BETA*H(NX-1)**2D0
#      *(H(NX-1)*HXX(NX-1)/(2D0*DX)+3D0*HX(NX-1)*HXX(NX-1)
#         -H(NX-1)*HX(NX-1)/DX**2D0))
  CW(NX-1)=2D0*CC(NX-1)+H(NX-1)**2D0*HXXX(NX-1)*
#      (-H(NX-1)**2D0/(2D0*DX)+3*BETA*HX(NX-1)**2D0/DX-2*BETA
#      *H(NX-1)*HXX(NX-1)/DX +4*BETA*H(NX-1)*HX(NX-1)/DX**2D0)
  CWW(NX-1)=-CC(NX-1)
  DO 90 I=1,NX-1
       MWW(I)=BWW(I)+CWW(I)
       MW(I)=BW(I)+CW(I)+DW(I)+EW(I)
       MP(I)=AP(I)+BP(I)+CP(I)+DP(I)
       ME(I)=BE(I)+CE(I)+DE(I)+EE(I)
       MEE(I)=BEE(I)+CEE(I)
```

```
90      CONTINUE
        DO 100 I=1,NX-1
           DO 100 II=1,NX-1
              M(I,II)=0D0
100     CONTINUE
        M(1,1)=MP(1)
        M(1,2)=ME(1)
        M(1,3)=MEE(1)
        M(2,1)=MW(2)
        M(2,2)=MP(2)
        M(2,3)=ME(2)
        M(2,4)=MEE(2)
        DO 110 I=3,NX-3
           M(I,I-2)=MWW(I)
           M(I,I-1)=MW(I)
           M(I,I)=MP(I)
           M(I,I+1)=ME(I)
           M(I,I+2)=MEE(I)
110     CONTINUE
        M(NX-2,NX-4)=MWW(NX-2)
        M(NX-2,NX-3)=MW(NX-2)
        M(NX-2,NX-2)=MP(NX-2)
        M(NX-2,NX-1)=ME(NX-2)
        M(NX-1,NX-3)=MWW(NX-1)
        M(NX-1,NX-2)=MW(NX-1)
        M(NX-1,NX-1)=MP(NX-1)
        END

C -----SUBROUTINE TO FIND INVERSE A. (GAUSS-ADAM METHOD)   ---
        SUBROUTINE INVERSE(A,N,NM)
        DIMENSION A(NM,NM),IS(N),JS(N)
        DOUBLE PRECISION A,DD,T
        LOGIC=1
        DO 100 K=1,N
           DD=0D0
           DO 10 I=K,N
           DO 10 J=K,N
              IF(ABS(A(I,J)).GT.DD) THEN
                 DD=ABS(A(I,J))
                 IS(K)=I
```

```
                    JS(K)=J
                END IF
10          CONTINUE
            IF (DD+1.0D0.EQ.1.0D0) THEN
                LOGIC=0
                WRITE(*,*) 'PROGRAM FAILED'
                RETURN
            END IF
            DO 30 J=1,N
                T=A(K,J)
                A(K,J)=A(IS(K),J)
                A(IS(K),J)=T
30          CONTINUE
            DO 50 I=1,N
                T=A(I,K)
                A(I,K)=A(I,JS(K))
                A(I,JS(K))=T
50          CONTINUE
            A(K,K)=1.0D0/A(K,K)
            DO 60 J=1,N
                IF(J.NE.K) THEN
                    A(K,J)=A(K,J)*A(K,K)
                END IF
60          CONTINUE
            DO 70 I=1,N
                IF(I.NE.K)   THEN
                    DO 80 J=1,N
                        IF(J.NE.K) THEN
                            A(I,J)=A(I,J)-A(I,K)*A(K,J)
                        END IF
80                  CONTINUE
                END IF
70          CONTINUE
            DO 90 I=1,N
                IF(I.NE.K) THEN
                    A(I,K)=-A(I,K)*A(K,K)
                END IF
90          CONTINUE
100     CONTINUE
        DO 130 K=N,1,-1
```

```
            DO 110 J=1,N
                T=A(K,J)
                A(K,J)=A(JS(K),J)
                A(JS(K),J)=T
110         CONTINUE
            DO 120 I=1,N
                T=A(I,K)
                A(I,K)=A(I,IS(K))
                A(I,IS(K))=T
120         CONTINUE
130     CONTINUE
        RETURN
        END
```

VITA

The author, Qingfang Wu, was born in April 1975, in Zhejiang, People's Republic of China. She graduated from Yanzhou High School in July 1992. In September 1992, the author attended Xi'an Jiaotong University (XJTU) with a major in fluid mechanics. She obtained a Bachelor of Science degree in July 1996. She continued her graduate study in XJTU and obtained her Master of Science degree in fluid mechanics in May 1999. After that, she worked in Beihai Yinhe Hi-Tech Industrial Co., Ltd. for one year. In August 2000, the author enrolled in the Department of Mechanical Engineering at Louisiana State University. She did the master's research under the direction of Dr. Harris Wong. She expected to graduate with a master's degree in mechanical engineering from Louisiana State University in May 2003.